Electrochemical and computational studies of benzothiophene compounds as corrosion inhibitors of mild steel in 1 M hydrochloric acid

N.G CHIRWA

orcid.org **0000-0000-2824-6638**

Dissertation submitted in fulfillment of the requirements for the degree *Master of Science in Chemistry* at the North West University

Supervisor: M.E Mashuga

Graduation ceremony: 24 November 2022

Student number: 29226007

Declaration

I declare that this project which is submitted in fulfillment of the requirements for the degree of Master of Science in Chemistry (M.Sc.) at North West University, Mafikeng Campus has not been previously submitted for a degree at this university or any other university. The following research was compiled, collated, and written by me. All the quotations are indicated by appropriate punctuation marks. Sources of my information are acknowledged in the reference pages.

Nhlanhla Gift Chirwa

Acknowledgements

This study is not possible without good health. God has been with me in this journey without a doubt. So many times, I felt like giving up, but I always had the fortitude, thanks to my belief. Much appreciation also goes to my supervisor Dr Mashuga who demands no less than the best from me. My supervisor has kept me on my toes, often giving me important life advice as my professional supervisor. He has been like a father far from home, and I am eternally grateful for that.

The financial assistance I have received from NRF and NWU has been well appreciated. Without these entities supporting me, I would not have gotten this far. I also want to acknowledge the contribution made by the NWU chemistry department technicians who have assisted me with my experiments.

I am grateful to my Father, Lucky Nhlanhla Chirwa, and I can't imagine being a single father raising three kids. Things have been demanding since we lost my mother. Depression and physical sickness have hampered our family, but we draw strength from his strength. I appreciate your fatherly advice and nurturing. Love to my sisters, my older sister Simphiwe Valencia Chirwa and my baby sister Owami Melissa Chirwa. These two are my heart, and I can't live without them. I appreciate their encouragement and love.

To my friends who have supported me in my studies during my time in NWU, great friends for life who I have met in my journey, thank you Vuyani Mokoko, with much appreciation for your assistance and just being there for me in my dark and good times.

Abstract

In the study, five benzothiophene derivatives were used as corrosion inhibitors for mild steel in a 1 M hydrochloric acid solution. The molecules have the same benzothiophene ring and only differ in the substituents attached to the ring. The study investigated their anti-corrosion and adsorption capabilities on mild steel in an acidic medium. Electrochemical, quantum chemical, spectroscopic, and adsorption isotherms techniques were used to evaluate the inhibitors for anti-corrosion properties. Careful examination of the Tafel and EIS analyses showed that the inhibitors exhibited good inhibition efficiency, and the following order of the inhibitors was reported: B5 > B2 > B3 > B4 > B1. The Tafel analysis showed that most of the inhibitors functioned as mixed-type inhibitors (interacting with both the anodic and cathodic reactions). The exception was B4, which mainly acted as a cathodic inhibitor. The EIS analysis showed that the benzothiophene derivatives exhibited high corrosion resistance levels by forming a passive film on the mild steel surface to shield the alloy from corrosion. The benzothiophene inhibitors also obeyed the Langmuir adsorption isotherm with their R^2 values near to unity. The ΔG°_{ads} values for four inhibitors were less than -20$kJ\ mol^{-1}$, suggesting the inhibitors were interacting with the mild steel via physisorption. The only exception was B5 which exhibited values between the range of -20$kj\ mol^{-1}$ to 40 $kJ\ mol^{-1}$, which meant the inhibitor interacted with the metal via physisorption and chemisorption.

The computational study produced promising highest occupied molecular orbital and lowest unoccupied molecular orbital figures which showed that the benzothiophene ring and the substituents could donate and receive electrons. The calculated parameters showed that the molecules all have the potential to interact with the metal surface. The order of decreasing E_{HOMO} was observed to be B1 > B3 > B2 > B4 > B5, which showed B1 with the highest electron-donating ability. The decreasing order of E_{LUMO} was determined to be B1 > B2 > B3 > B5 > B4. The trend was not aligned with the experimental inhibition efficiencies, which suggested that the inhibition potentials of the inhibitors were entirely informed by their ability to receive electrons from the occupied orbitals of Fe. The decreasing order of the energy gap was shown to be B1 > B2 > B3 > B5 > B4. B4 had the lowest reported energy gap in the study. However the difference in the energy gap values were not significant, indicating that the inhibitors exhibited high levels of reactivity.

Keywords: Benzothiophene derivatives;corrosion inhibitor; mild steel; electrochemical methods; density functional theory

List of abbreviations

AC	Alternating Current
AD	Anno Domini
BC	Before Christ
B3LYP	Becke, 3-parameter, Lee-Yang-Parr
CE	Counter Electrode
DFT	Density Functional Theory
EIS	Electrochemical Impedance Spectroscopy
FTIR	Fourier Transform Infrared Spectroscopy
GDP	Gross Domestic Product
HOMO	Highest Occupied Molecular Orbital
IE	Inhibition Efficiency
LSV	Linear Sweep voltammetry
LUMO	Lowest Unoccupied Molecular Orbital
MO	Molecular Orbital
MS	Mild Steel
AMPP	Association for Materials Protection and Performance
OCP	Open Circuit Potential
Ppm	Parts per million
PDP	Potentiodynamic Polarization
RE	Reference Electrode
WE	Working Electrode

List of figures

List of tables

Table of contents

Chapter 1

Introduction

1.1 Background and motivation for study

"War seems to come out of nowhere, like rust that suddenly pops up on iron after a storm." This famous quote was once uttered by Victor Davis Hanson. Nevertheless, no one can doubt that Mr Hanson's quote was a reference to the volatility and suddenness of war. It is not that much different from the war humanity currently has with rust, an almost invisible and unnoticed war wreaking havoc on our society and economy. Rust is naturally a by-product of a complex chemical process known as corrosion. Corrosion has many definitions, some specific to a type of corrosion and some broader to cover different forms of corrosion. The word corrosion originated from the Latin corrodere, which means to "gnaw to pieces." In modern times, however, the public defines corrosion as the gradual deterioration of a material caused by its surface being eaten away. Academics, however, define corrosion as the destruction of a material's physical properties caused by its chemical reaction with its environment [1]. Corrosion affects many aspects of our lives, both direct and indirect. The loss of personal property incurred by corrosion can be considered, a direct effect. Manufacturers, producers, and suppliers of goods and services usually experience a loss of materials due to corrosion leading to higher consumer prices, which is an example of corrosion indirectly affecting the public. The phenomenon of corrosion affects a torrent of industries such as mining, petrochemicals, electronics, and manufacturing, to name a few [2]. Most metals and alloys undergo corrosion with only a few exceptions. Corrosion adversely affects a material’s structural integrity and causes discolouration on a metal's surface. A corroded metal or an alloy is considered useless in most industries. It does not help that most metals are not thermodynamically stable and readily react with any substances in their proximity, such as air, water, acids, bases, and other gaseous substances.

1.2 Problem statement

Corrosion often has profound financial implications, so it is no surprise that numerous studies have been conducted to monitor the ecological and economic damages incurred by corrosion. According to the Association for Materials Protection and Performance (AMPP), the global economy sheds an excess of four trillion dollars yearly on corrosion, an equivalent of regression on our global GDP of four percent annually. In South Africa, the annual corrosion damage is estimated to be around 9.6 billion dollars [3]. Corrosion affects several economically essential industries, but it is most prevalent in manufacturing, transportation, and construction. What these industries have in common is their extensive use of mild steel. Mild steel is a low-carbon alloy composed of copper, carbon, silicon, and manganese, with iron making up 99% of the composition. The primary issue of mild steel is its high susceptibility to corrosion in most environments, primarily believed to be because of its high iron content. Iron is known to be stable as an oxide and is mined as ore termed hematite. Once separated from impurities like oxygen using processes such as carbon reduction, iron stability is significantly reduced. Mild steel's high iron content makes the metal very prone to rust. For this reason, the metal alloy requires additional protection in the form of corrosion inhibitors that produce a layer of protection on the surface of the alloy. The cost of corrosion is not limited only to finance. The ramifications are sometimes much more grave. One such harrowing case was the Bhopal gas tragedy in India on December 2^{nd} -3^{rd} 1984 when 2,259 lives were lost, and over 500 000 more were exposed to isocyanate gas and other chemicals. Researchers and

investigators concluded that the cause was a gas leak due to a corroded pipeline. The Guadalajara explosions are also an unfortunate example of the dire effects of corrosion. On April 22nd, 1992, several gasoline explosions in the sewer systems led to the death of 252 people, with 500 injured, and 15000 left homeless. The event's investigation attributed the disaster to a galvanized water pipe that was subjected to stray current corrosion. The pipe seeped water onto a gasoline pipe which underwent aqueous corrosion and eventually caused fatal explosions [4]. Corrosion sometimes seems unavoidable, but it can often be avoided when proper precautions and preventive measures are consulted.

1.3 Justification of the study

Technology is advancing at a fair pace almost every year. The world has new and exciting technology that shortens the period between the present and the future. Amid the fourth industrial revolution, the stride of technology is not nearing a plateau. The common mineral for industrilasation and urbanisation has always been metals. Metals are the foundation of modern civilisation, buildings, transportation, and electricity, for example. Modern society is not feasible without metals, yet our efforts in protecting these vital minerals have been far from adequate. Corrosion resistance has received considerable attention, but not nearly enough. Corrosion resistance is often relegated to less importance when materials are chosen to produce specific properties, such as strength, durability, and electrical conductivity. The consequence of this practice is that corrosion now occurs in almost every industry, from microelectronics and civil structures to everyday items in our mundane lives. It is, therefore, important that humanity takes significant steps towards understanding the nature of corrosion. Contemporary methods of mitigating corrosion are hazardous to the environment and its inhabitants, whether it be toxic zinc fumes from galvanisation causing illness in Louisiana, electroplating wastewater that threatens water safety and marine life, or toxic inhibitors poisoning the air [5-7]. The need for cost-effective, eco-friendly ways of mitigating corrosion is very important. Fortunately, organic corrosion inhibitors have been getting much attention in the search for practical and environmentally friendly corrosion inhibition methods. The benzothiophenes inhibitors investigated in this study show considerable potential as effective environmentally friendly corrosion inhibitors.

1.4 Research questions

Metals are rarely found in their typical metal form. Metals are found in rocks in their stable condition, known as metal oxides or ores [8]. Corrosion results from an intrinsic property of metals to revert to their stable ore state. Mild steel is an alloy composed mainly of iron and carbon. The iron in mild steel can readily react with oxygen to form iron oxide or ore with little to no effort. The current study aims to find the answer to whether it is possible to mitigate a natural phenomenon such as corrosion, and if so, what approaches can be taken to reduce corrosion using benzothiophenes molecules as inhibitors.

1.5 Aim and objectives

The aim of the study is to test the potential of some benzothiophene derivatives as corrosion inhibitors of mild steel in 1 M hydrochloric acid, using electrochemical, spectroscopic, and quantum chemical studies.

The objectives are:

- Study the effect of concentration on the corrosion inhibition of benzothiophene inhibitors on mild steel corrosion in 1 M HCl solution using electrochemical methods.
- Investigate the mode of adsorption and interaction of the studied benzothiophene derivatives on the mild steel surface in an acidic medium using both electrochemical and spectroscopic method.
- Determine the effect of the molecular structure on the corrosion inhibition efficiency of the benzothiophene derivatives and the assessment of the structure-activity relationship,
- Perform quantum chemical calculations on the benzothiophene derivatives to correlate the quantum chemical parameters with the experimental inhibition efficiencies of the compounds.

1.6 Research hypothesis

Several scientific papers have reported the excellent corrosion efficiency and cost-effectiveness of compounds containing phosphorus, oxygen, and nitrogen. The benzothiophene molecules in the study possess sulphur along with various heteroatoms in their structural ring. The presence of the conjugated benzothiophene ring with pi-electrons and heteroatoms makes benzothiophene inhibitors prime targets for corrosion inhibition [3, 9, 10]. Aromatic rings are known for donating electrons from their pi-electrons to metallic cations. For that reason, it can be inferred that the benzothiophene molecules in this study have the potential to inhibit metal corrosion.

1.7 Scope of the study

Five benzothiophene derivatives were used as corrosion inhibitors in a 1 M HCl acid solution. The molecules were selected by examining their structural properties, potential abilities to inhibit corrosion and their novelty. The methods used to investigate their anti-corrosion properties were, but not limited to, electrochemical, quantum chemical calculations and spectroscopic techniques.

Chapter 2

Literature review

2.1 Historical background

The term corrosion seems to be nearly as old as the earth itself. The word has appeared in several texts, including the famous word in the bible in the book of Matthew [11]. Corrosion has been around since antiquity, known all around the globe by different monikers. In modern times, however, corrosion is commonly known as rust. Contrary to mainstream belief, corrosion is not only limited to metallic materials but almost all materials in general, such as plastics and ceramics. However, when the phenomenon occurs in non-metallic products, its often referred to as degradation. Scientists, philosophers, and writers of antiquity all have a historical account of corrosion in their respective texts [1]:

- Pliny the Elder, in AD 23-79, penned a passage about spoiled iron.
- Herodotus, in the fifth century (BC), proposed using tin to protect iron from corrosion.
- Robert Boyle wrote the famous book, mechanism of corrosion, that, delved into the mechanism of corrosion.

The pivotal discoveries on corrosion were later made by the physicist and father of electricity, Michael Faraday. In the period 1791-1867, Faraday was able to form a measurable connection between chemical action and current. Faraday proposed some laws that would later be the foundation for the modern determination of metal corrosion rates [12]. The nineteenth century ushered in an era rich with bright and novel ideas about corrosion control methods. In 1903, Willis Rodney Whitney characterised corrosion as an electrochemical phenomenon while the scientific community was still unaware of the nature of the process [13]. The mid and late 1900s saw the emergence and advancement of techniques used to study corrosion. To this day, corrosion remains a considerable problem, and progress in controlling it appears to be gaining traction.

2.2 Basics of corrosion

Corrosion is predominately an electrochemical phenomenon. It usually involves at least two reactions occurring on the surface of the corroding metal. Oxidation (anodic reaction) and reduction (cathodic reaction) can either occur over the entire surface of the metal, which would lead to uniform corrosion, or they can take place in isolated areas on the metal surface to cause localised corrosion [14]. The mild steel investigated in the study is a metal mainly composed of iron and carbon. Electrochemical reactions that occur when iron rusts are shown in figure 2.1 [15].

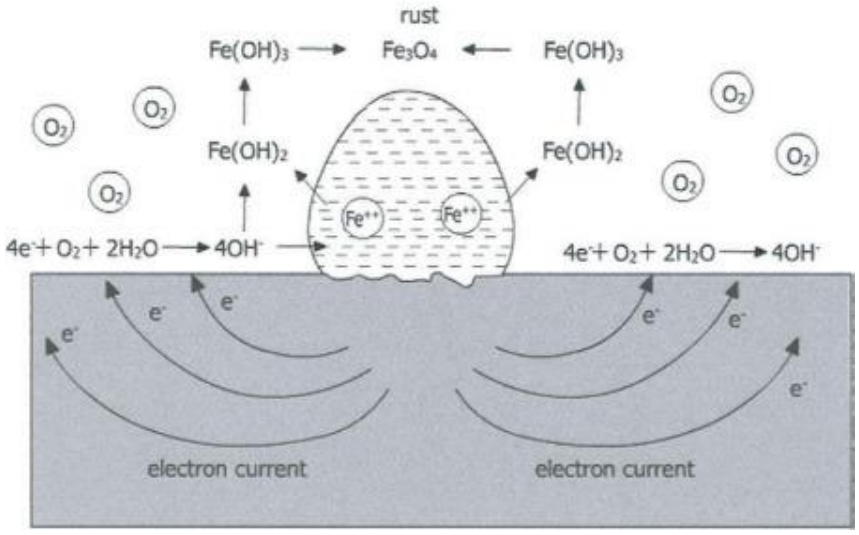

Figure 2.1 Process of iron corrosion [16].

In the anodic area, the oxidation of the metal takes place

Fe→ Fe^{2+} +2e^{-}.

In the cathodic area, reduction of oxygen occurs

2H_2 O + O_2 + 4e^{-} → 4OH^{-}

The hydroxyl ions react with the ferrous ions produced at the anode giving the reaction:

Fe^{2+} + 2OH^{-} → Fe$(OH)_2$

Subject to oxygen availability in the air, Fe$(OH)_2$ will oxidise to produce Fe$(OH)_3$ and, in the process, lose water:

4Fe$(OH)_2$ +O_2 +2H_2 O→ 4Fe$(OH)_3$

Fe$(OH)_3$ will be converted to hydrated ferric oxide(rust) by oxygen:

4Fe$(OH)_2$ +O_2 → 2Fe_2O_3.H_2O +2H_2 O

2.3 Types of corrosion

Mild steel is the metal of choice by many vital industries due to its inexpensiveness and excellent mechanical properties. It poses a significant problem when that same metal exhibits poor corrosion resistance [17]. Mild steel is highly susceptible to corrosion in typical usage environments. There are different types of corrosion, such as [11, 18]:

- Uniform corrosion occurs when an entire material's surface is exposed to a corrosion current leading to a reduction in the thickness of the material. Uniform corrosion is the most common form of corrosion.
- Pitting corrosion occurs when localised pits appear on the metal surface, usually induced by the local depassivation of an area.
- Crevice corrosion is a type of corrosion that involves a localised attack on the aperture of metallic materials. It is caused by shielding on the metallic surface, preventing contact with the surrounding environment.
- Galvanic corrosion involves an electrochemical process between metals resulting in one metal corroding when in contact with another metal. It usually occurs when both metals are immersed in an electrolytic solution like water.
- Corrosion fatigue is a form of corrosion that occurs when a metallic component in a corrosive media is subjected to cyclic stress.

2.4 Corrosion prevention methods

Corrosion has been a problem to civilisation for ages, from damaging infrastructure to affecting transportation. Scientists have come up with ways to limit corrosion damage with varying success levels. The science of corrosion protection has come a long way from the days of antiquity when hot-dip galvanization was discovered [19]. In recent times, however, the corrosion protection industry is amidst a balancing act. The goal today for scientists is to come up with environmentally-friendly and practical techniques to limit or prevent corrosion at a reasonable financial cost. So, it is no surprise that today the most common method of corrosion prevention is protective coatings such as paint, powder, and plastics. These techniques are easily accessible and cost-effective [20-22]. The disadvantage of barrier coatings is that they need to be constantly replaced and are usually composed of very toxic substances [23, 24]. Early forms of corrosion protection revolved around coating the desired metals with other metallic materials to shield them from corrosion. These methods were galvanisation and electroplating. Galvanisation is a process where a metal is protected from corrosion by embedding another more reactive metal such as zinc. The elements quickly oxidise the surface metal, zinc, while the metal underneath remains undamaged. The process is classified as sacrificial protection as the zinc functions as a sacrificial anode interacting with the harsh environment [25, 26]. Hot-dip galvanisation is the most common method of galvanising. It involves dipping metal into molten zinc, to enable the zinc to tightly bind to the metal. The galvanisation process is quite to set up, and the apparatus required is not practical either, as there is a limit to the size of the material to be coated. The process also damages the environment due to the highly toxic zinc fumes [27-29].

Electroplating involves coating the desired metal by covering it with another material less prone to corrosion. Electroplating consists of using electrolysis to coat a metal with another material to prevent it from corrosion in a process called electrodeposition [30]. Electroplating is used today to protect and, sometimes enhance, the aesthetic appeal of materials. The downside of electroplating is the cost of setting up the machines that run the process, and the waste from the process is usually harmful to the environment [31, 32]. Another form of corrosion protection is electrochemically

passivating active sites on the metal surface. This process is known as cathodic protection and is achieved by using galvanic anodes (zinc, magnesium, aluminium.), which provide electrons to active areas of the metals to passivate the sites and prevent corrosion [33]. Although cathodic protection is a highly effective method for corrosion protection, it does have its drawbacks. For one, the galvanic anodes do not last for a long time and have to be constantly replaced, which drives up the maintenance costs. The technique is also less effective in high resistance conditions [34].

Corrosion chemistry is progressing at a breakneck pace, and every chemical process is subjected to detailed investigations to examine its safety, environmental impact, and cost. With the number of corrosion protection methods available in modern times, the use of inhibitors has garnered some strong attention. Corrosion inhibitors are substances that, when added to corrosive conditions, either stop corrosion or slow down the process. The use of inhibitors is an old process, as early as the mid-19th century inhibitors were used for acid pickling of rust. In antiquity, corrosion inhibitors employed in acidic conditions were usually raw materials and processed products of plants and animals, namely vegetable oil, gelatin, and syrup. It was not until the 20th century that corrosion materials shifted from natural products to minerals such as chromate, silicate, nitrate, and coal tar. The era was regarded as the pivotal period for corrosion inhibition technology in the mid-1930s when synthetic organic inhibitors were used on materials in acidic conditions. In that same period, inorganic inhibitors were also increasingly used on materials in neutral conditions, such as seawater and industrial water. Research and development on corrosion inhibitors were greatly enhanced with their growing use in the industry, much was uncovered about their inhibition mechanisms. Concepts such as physical adsorption, chemical adsorption, and integrated adsorption theory were proposed in the 1950s. Scientists devoted a great deal of time researching inhibitor molecule design in the 1960s, which promoted the inhibitor theory's development. The proliferation of several high-performance corrosion inhibitors used in the industry followed. The worsening pollution caused by the industry led to a probe into the use of inorganic inhibitors in the 1970s. The use of toxic high polymer corrosion inhibitors drove scientists to search for cleaner and safer inhibitors in the fight to counteract pollution. In their search, scientists started using organic corrosion inhibitors, which have proved to be a viable and safer alternative to other corrosion inhibition methods [35].

2.5 Electrochemical Characterization methods

The process of characterising an electrochemical reaction requires the setup of an electrochemical cell. The cell in this study involves the use of three electrodes which are the working electrode (WE), reference electrode (RE), and counter electrode (CE). An electrochemical cell consisting of four electrodes may also be observed. In this study, however, the three-electrode system was employed with the metal (mild steel) acting as the working electrode. Furthermore, a counter electrode was involved as the electrode required to close the electrical circuit. The reference electrode performed the task of measuring the working electrode’s potential. All three electrodes were submerged in an electrolytic solution of 1 M HCl with and without the inhibitor. Figure 2.2 shows a schematic diagram of the three-electrode system [36].

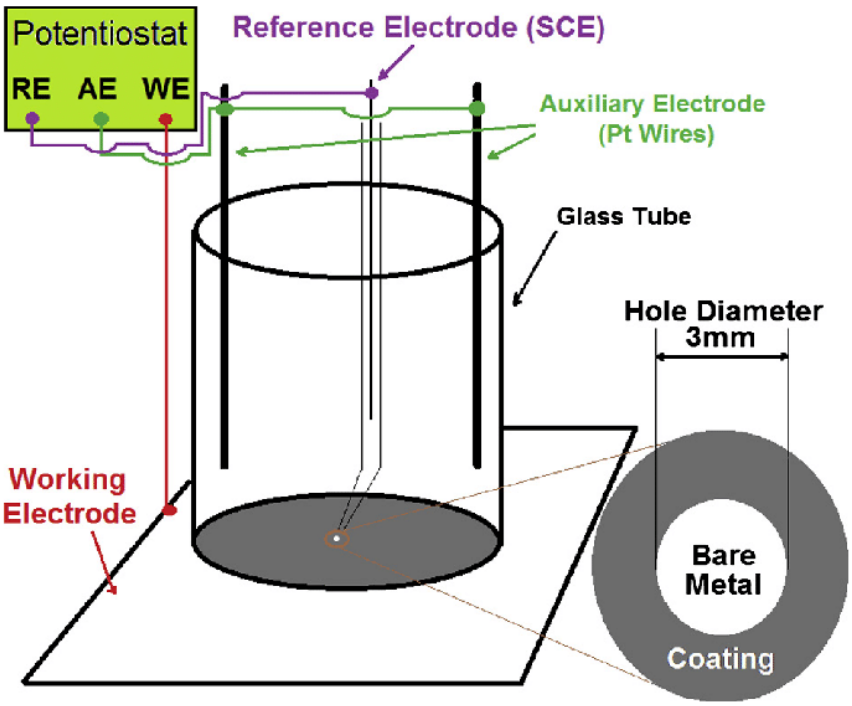

Figure 2.2. Three electrode electrochemical cell

The system is given time to stabilize for 30 minutes until a steady open circuit potential (OCP) is reached. After that, measurements of the Tafel polarization (PDP) and electrochemical impedance spectroscopy (EIS) can be done.

2.5.1 Linear sweep voltammetry (LSV)

Linear sweep voltammetry is one of the most common techniques for corrosion determination. The potential of the working electrode is swept to determine and observe the current response. The technique helps attain crucial data in various corrosion systems, such as the corrosion rate and mechanism. The method can also determine varying levels of corrosion resistance different materials possess in multiple environments [37]. LSV is a unique and crucial electrochemical method that employs a solid electrode and is characterized by its fixed potential and fast scan properties. Units of volts per minute denote the slope of an LSV, commonly called the experiment's scan rate [38]. The determination of the corrosion rate involves the kinetics of the oxidation and reduction reactions. Faraday's law implies a linear relationship between the corrosion rate (Rm) and the corrosion current(i_{corr}) [11].

$$R_M = \frac{M}{nF\rho}\ i_{corr} \quad , \tag{2.1}$$

where the atomic weight of the metal is denoted as M, the density is indicated as ρ, n represents the charge number that accounts for the number of electrons exchanged in the reaction, and the Faraday constant is characterised as F with a value of (96.485 C/mol).

The determination of the corrosion rate involves the formation of corrosion currents. When the reaction system for the corrosion reaction is observed or known, a Tafel slope analysis is employed to determine the corrosion currents[39]. Contemporary theories of aqueous metallic corrosion are currently based on electrode kinetics. For a corrosion system involving an anodic and cathodic reaction, applying the Butler-Volmer equation and the mixed potential theory will yield the following equation[40]:

$$I = i_{corr} \left(e^{2.303 \frac{n}{b_a}} - e^{2,303 \frac{n}{b_c}} \right) \quad (2.2)$$

$$\eta = E - E_{corr} \ , \quad (2.3)$$

where E denotes the applied potential, the current density is denoted by I, and η represents the system over potential, which results from a difference between the applied potential and the corrosion potential (E_{corr}). Corrosion potential and current density are denoted by E_{corr} and $i_{corr,}$ respectively. The corrosion potential is also known as the open circuit potential and is obtained when the metal is undergoing corrosion. The anodic and cathodic Tafel slopes are denoted by b_a and $b_{c,}$ respectively, along with the current density obtained from experimental data.

High anodic overpotentials can also be represented by a η/b_a value larger than 1. The Butler-Volmer are simplified to give the following equation:

$$\eta = \log (i_{corr}) + b_a . \log(i). \quad (2.4)$$

However, if a high cathodic over potential is observed or a η/b_c value lower than -1 is recorded, the Tafel equation for the reaction of the cathode is explained by the following equation:

$$\eta = \log (i_{cor}) - b_c . \log|i| \ . \quad (2.5)$$

The Tafel equations above yield a straight line representing the difference of the logarithm of current density with potential; this results in the currents being shown as semi-logarithmic plots termed Tafel plots. Scientists employ a Tafel analysis to generate corrosion data, such as the corrosion rate. This mode of analysis is known as the Tafel slope analysis. Figure 2.3 is a diagram representing a quintessential Tafel slope analysis [41].

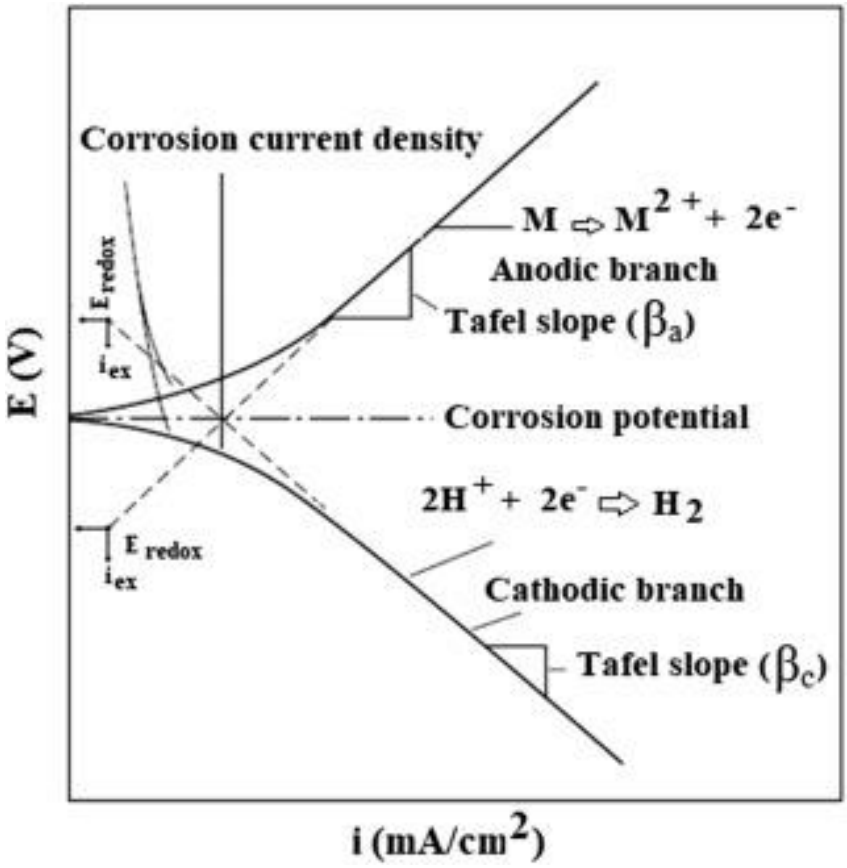

Figure 2.3 Tafel slope diagram [41].

The corrosion current (i_{corr}) values obtained from the Tafel slope are used to determine the protection or inhibition efficiency with the use of the following equation:

$$\%IE_{PDP} = \frac{i^{\circ}_{corr} - i_{corr}}{i^{\circ}_{corr}} \quad (2.6)$$

where i°_{corr} represents the current density for the system without the inhibiting compound, and i_{corr} represents the current density of the solution containing the inhibitor at various concentrations.

2.5.2 Electrochemical Impedance Spectroscopy (EIS)

Electrochemical impedance spectroscopy has amassed a fair amount of notoriety in contemporary science. Initially, the technique was primarily employed when determining the double-layer capacitance and alternative current (AC) polarography [42]. In recent times, however, the technique has become essential for characterising electrochemical systems and complex interfaces.

With the use of EIS, scientists can represent a variety of materials, including but not limited to coatings, electronics, ceramics, and fuel cells [43]. EIS has found considerable use in studying mechanisms in electrodeposition, electro dissolution, passivity, and corrosion phenomena. The technique examines a corrosion system's response to the application of a periodic small amplitude AC signal. The measurements are conducted at various AC frequencies hence the name impedance spectroscopy. The advantages of using the method over alternative methods such as DC are: (i) since the process is a linear technique, results are promptly and efficiently attained in terms of the linear systems theory; (ii) when determined over an infinite frequency range, the impedance carries all the data that can be drawn from the system by the use of linear electrical perturbation/response techniques;(iii) the high levels of data that is transferred from the observer in comparison to the amount of data that is generated by the experiment [44].

The impedance technique principle involves applying a small amplitude excitation signal to the system undergoing investigation. The response is compared with the applied signal by measuring the current and voltage phase shift by determining their amplitudes. The applied excitation signal is in the form of sinusoidal disturbance potential (ΔE), which is imposed under steady-state conditions in the system. The current response is a sinusoidal current (ΔI) with a phase difference (φ) from the initial disturbance. Consequently, the impedance, denoted by Z, measures the relationship between ΔE and ΔI.

The EIS method functions in the frequency domain. It is established that an interface is observed as an amalgam of passive electrical circuit elements such as capacitance, resistance, and inductance. Ohm's law is the result when AC is applied to the elements. With the use of EIS, the data concerning the mild steel/inhibitor and the HCl corrosion system can be attained, such as the surface electrochemical properties of the mild steel and inhibitors. In addition, the surface film of the metal is also observed along with the electrochemical interactions between the metal, its medium, and the inhibitors [45].

EIS determinations are often elucidated using the relationship between the impedance data and equivalent circuits delineating the physical processes occurring in the system of interest through graphical representations.

A graph of Z= $Z' + Z''$(where Z' and Z'' are the real and imaginary parts) measured at different frequencies generates a Nyquist plot. Another graphical representation called a bode plot is also produced. The bode plot depicts the logarithm of impedance modulus (log|Z|) and the phase displacement as a function of the frequency logarithm. The Nyquist plot contains a series of points, which individually represent the magnitude and direction of the impedance vector of a specific frequency [46, 47]. A Nyquist plot is composed of a complex plane of Cartesian coordinates, where the real part(abscissa) of impedance and the imaginary part of impedance(ordinate) are plotted on a Cartesian plane under different frequencies with the scale of 100 kHz to 10mHz. Figure 2.4 represents a classic Nyquist plot and its equivalent circuit [48].

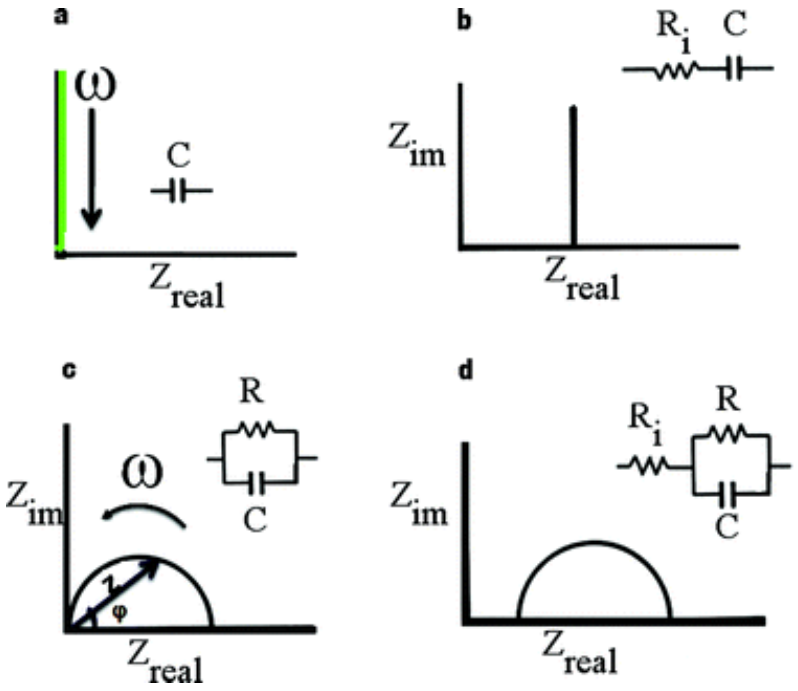

Figure 2.4 A typical Nyquist plot and its equivalent circuit.

A Nyquist plot like the one above in Figure 2.4 is subjected to a fitting to generate an equivalent circuit. The circuit contains essential data about the mechanism or process of corrosion for the current study. The right side of the semicircle observed on the Nyquist plot is extrapolated to identify the horizontal axis. The diameter of the extrapolated semicircle in the Nyquist plot is the charge transfer resistance (Rct). The system solution resistance and constant phase element (Q,Y_o) are some parameters that can be extracted from the equivalent circuit. The charge transfer (R_{ct}) value obtained from the circuit is used to calculate the protection efficiency of the inhibitor using the following equation:

$$\%IE_{EIS=}\left(1-\frac{R_{ct}^{\circ}}{\text{Rct}}\right)\times 100 \qquad (2.7)$$

where R_{ct}° represents the charge transfer resistance for the uninhibited system, and R_{ct} represents the charge transfer resistance for the concentrated systems.

2.6 Benzothiophene synthesis

Benzothiophene is generally observed as a core structure to biologically active compounds such as raloxifene and sertaconazole. Figure 2.5 shows a more efficient method for benzothiophene synthesis.

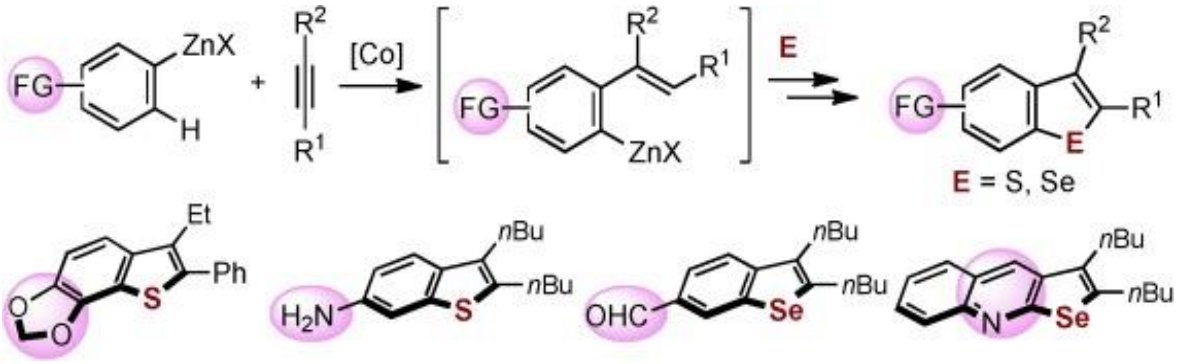

Figure 2.5: Diagram of the benzothiophene synthesis scheme

The scheme above combines cobalt-catalysed migratory arylzincatiom, and copper-mediated/catalysed chalogenative cyclisation, producing a benzothiophene ring from analyzing reagents, alkynes, and elemental chalcogens. Benzothiophenes and benzoselenophene, diversely functionalised at the benzene ring moiety, can be synthesised since they are not readily accessible by conventional methods [49]. A method of benzothiophene synthesis, developed by Singh and colleagues in 2016, involves the formation of the benzothiophene skeletons via arynes intermediates and further added with the aryne intermediates (fig 2.6). The benzothiophenes are synthesized from aryne precursors and alkynyl sulfides. A nucleophilic attack on the sulfur or carbon of alkynyl sulfides to electrophilic aryne intermediates occurs, followed by ring closure (fig 2.6 D) [50].

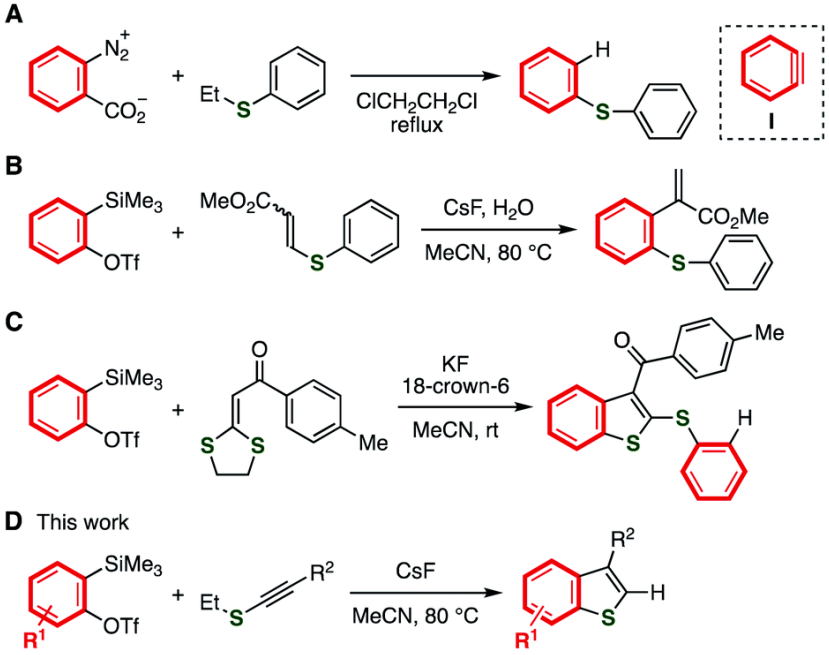

Figure 2.6 Diagram of the benzothiophene synthesis scheme

Benzothiophene is an organic heterocyclic compound with a chemical formula not unlike its close cousin naphthene, which it produces an odour similar to. The benzothiophene group are an influential group of compounds exhibiting several biological functions. The compound and its related derivatives are renowned in the scientific community as pesticides, fungicides, and herbicides [51, 52]. The structure of benzothiophene is seen as a perfect scaffold in the production of biodynamic agents [53]. A number of the derivatives are often used in the pharmaceutical sector as estrogen receptor antagonists. They are also modulators of multidrug resistance and anti-hypersensitive, antibacterial, antilaxative, antiviral, anticancer, and anti-inflammatory agents.

The derivatives are also employed as precursors for the production of much more complex heterocycles. Benzothiophene and its related derivatives are essentially sulphur containing heterocyclic compounds. The electron pairs on the sulfur atoms are localized in pi-conjugated systems. Benzothiophenes and their derivatives are generally found in petroleum or coal and are known because of their apparent therapeutic properties in medicinal chemistry [54].

2.7 Benzothiophene as corrosion inhibitors

In searching for viable and efficient corrosion inhibitors, scientists commonly investigate organic compounds containing heteroatoms, heterocycles, and pi-electron functional groups. Benzothiophene and its related derivatives meet the earlier mentioned criteria as they are heterocyclic organic compounds composed of hetero-atoms, namely sulphur and some other hetero-atoms found as part of the benzothiophene derivatives. The observed order of anti-corrosion strength of heteroatoms is O<N<S<P [3]. The heteroatoms generally have higher basicity and electron density than other atoms so that they can donate electrons to the vacant d-orbitals of the metal to form a covalent bond. The heteroatoms function as active areas for the adsorption of the inhibitor molecule on the mild steel surface. Studies show that most organic molecules adsorb on the metal surfaces by displacing water molecules on the metal surface to form a passive film [55]. The previously mentioned process is determined by the availability of non-bonded (lone pairs) and p-electrons in the inhibitor compounds. Electrons pass from the inhibitor to the metal surface to produce coordinate covalent bonds. The strength of the covalent bond is facilitated by the degree of electron density, the donor atoms of the functional group, and the polarisability of that group.

The sulphur atom is known for its adsorption properties on metal surfaces by replacing the water molecules on the metal surface [56]. The sulphur containing benzothiophene compounds possess a feature that makes them desirable targets for corrosion inhibition based on a theory of hard and soft bases (HSAB), which Pearson and Songstad introduced in the early 1960s [57]. According to the theory, substances containing sulphur atoms in their molecular structure are considered soft bases. The implication is that soft bases have low levels of electronegativity, which grant them the ability to easily donate electrons to metal surfaces because they cannot prevent electron cloud polarisation [58]. In addition to the present electro atoms such as oxygen and sulphur, the study will comprise of benzothiophene derivatives with halide atoms such as chlorine, bromine, and iodine. A number of studies on the effect halide atoms have on corrosion have been done. Observed

data indicates that halides inhibit the corrosion of some metals in strong acids. This effect depends on the ionic size and charge of the anion in the adsorption sites, and the nature and concentration of the halide ion. Halides have been known to inhibit and accelerate the corrosion of metals in acidic solutions [59].

It has been found that halide ions can improve the adsorption strength of organic actions by forming intermediate bridges between the positively charged metal surface and the positive end of the organic inhibitor, coupled with the pi-conjugated groups found in the benzothiophene heterocyclic ring. The inhibitory effects of the benzothiophene rings attached to halide atoms show great promise in corrosion inhibition studies [60]. The obvious medicinal applications of benzothiophene derivatives show their non-toxic nature, which is desirable in contemporary science since they will cause no harm to nature and humans.

Studies on the nature of benzothiophene and its derivative as corrosion inhibitors are scarce. Below are just some of the studies done on the compounds:

One such study used Tafel extrapolation and weight loss techniques to characterize and analyze the compound. The study was conducted in four temperature (C) ranges. It was concluded that the inhibition is governed by the physisorption mechanism. The results showed a strong linear relationship between the results of the inhibition efficiencies of the Tafel extrapolation and the weight loss techniques. The Tafel polarisation results showed a significant negative shift in the corrosion potential. The sizeable negative shift indicates the compound’s function as a competent cathodic inhibitor.

Another study reported the corrosion inhibition properties of several compounds, including benzothiophene-3-carbohydrazide(CBTC), for an aluminium alloy in a hydrochloric acid medium. Using weight loss measurements and polarization techniques, it was observed that CBTC had good inhibition efficiencies. The compound recorded a maximum inhibition efficiency of 87.03 % and the lowest efficiency of 77.81%. The compound adsorbed on the aluminium alloy surface to produce a passive film, and it was confirmed to have obeyed Temkin s and Langmuir's adsorption isotherms. The study suggests that the compound adsorbed on the metal surface through sulphur, oxygen, and nitrogen atoms to produce donor-acceptor interactions between its unpaired electrons of these atoms and the positive centers of the aluminium's surface. The corrosion inhibition was believed to be controlled by a physical adsorption mechanism [61].

2.8 Quantum chemical methods

Quantum chemical methods are a tried and tested chemistry method with a proven track record in the interpretation of a molecule's structure and its associated reactivity. Quantum chemical methods are a proper technique employed by chemists to investigate the efficiency of potential corrosion inhibitors by assessing the molecules' reaction mechanisms and electronic structure to determine their respective parameters. The Parameters are then used to screen chemical species with specific desired properties known to be of use in corrosion inhibition studies [62, 63]. The reactivity of an inhibitor is associated with its frontier molecular orbitals, a collective term for the highest occupied molecular orbital and the lowest unoccupied molecular orbitals. Other important

parameters that are also investigated, include the dipole moment, and the Lewis/ base hardness and softness of the molecule [63].

The density functional theory (DFT) has become a popular tool for determining a molecule's properties and energetics at a very reasonable cost [64]. The now broadly used method has recently been applied to materials science. The technique is used to design and develop organic inhibitors. The process is time and money saving compared to the known techniques used to discern inhibition mechanisms. DFT produces accurate and simple results for even the most complex systems at a meager cost. With DFT, chemists can understand the reactivity behaviour in terms of hard- and soft-acid/base (HSAB) theory which offers a more organised and systematic option for studying and forecasting the inhibitor/surface interaction.
Erwin Schrodinger, a famous Austrian scientist, proposed an equation that is the fundamental source of contemporary quantum chemistry [65]. The equation was an essential basis for elucidating any system's wave function. The formula in equation 2.8 is known as the Schrodinger equation and is observed to be independent of time. For a time-dependent system, equation 2.8 is better adapted for utilisation, and it also depicts a particle of mass(m) with energy(E) in motion in one dimension. The following equation is the Schrodinger equation:

$$-\frac{\hbar}{2m}\frac{d^2\varphi}{dx^2}+v(x)\varphi=E\varphi \ . \qquad (2.8)$$

V(x) represents the particle's potential energy at point x, while E. $\hbar=h2\pi$ denotes the system's total energy. $\hbar$ is a the modified Planck's constant with a value of 1.055×10^{-34} Js. The Hamiltonian operator and wave function depend entirely on the coordinates of all particles in a molecule. All molecules involved in a system are equally important. The resolution of the Schrodinger equation can determine the wave function expression and related energy value of a system. The application of the Schrodinger equation on the molecule leads to the discernment of atomic orbitals and molecular orbitals.

The use of quantum chemical methods to study corrosion inhibitors is conducted with the specific purpose of comparing the quantum chemical properties of the inhibitors with the inhibition potential of the molecule under investigation.

The geometries of the molecules are optimised and used for the DFT technique for corrosion studies. The hybrid exchange functional of Becke and the gradient corrected correlation function of Lee, Yang, and Parr, collectively known as B3LYP, are the density function used to study the molecules. In this current study, B3LYP, which is a type of DFT technique that utilises Becke's three-parameter functional B (3) and involves the mixture of HF with DFT exchange terms associated with gradient corrected correlation functional of Lee, Yang, and Parr (LYP). Will be employed in the study to conduct quantum chemical calculations. To determine the full geometry optimisations and vibrational analysis of the optimised structures of the inhibitor, the basis set of B3LYP/6-31G(d) is employed with the use of Spartan software to produce the quantum chemical parameters.

Quantum chemical methods produce a wide array of essential parameters. The E_{Homo},E_{lumo}, $\Delta E(homo-lumo)$ energy gap, electronegativity(x), Ionization potential, electron affinity

chemical potential(υ), chemical hardness(η), global softness(σ) and global electrophilicity(ω) are all crucial parameters generated by the DFT method [66].

Density functional theory remains a prevalent method of computational study because the technique requires less machine power from computers than other computational methods. The process favors electronic density over the wave function to calculate the energy forms [53-54]. A panoply of work has been done on DFT, making the technology accessible and much easier to use in corrosion studies. Computations on DFT are mainly conducted to investigate the electronic structure of the inhibitor molecules at an extensive range. The method can reveal the adsorption properties of the inhibitors by generating several quantum chemical parameters [55,56]. Below are examples of how chemical methods were used in corrosion inhibition.

The study of three amine derivatives (diethylenetriamine (I), triethylenetetramine (II), and pentaethylene hexamine(III) were conducted to protect carbon steel from corrosion. The DFT method was employed to determine the quantum chemical parameters. The HOMO and LUMO energies, hardness (η), and dipole moment (μ) were calculated and analysed. The results that showed compound (III) exhibited the highest inhibition potential. The combination had the highest E_{homo}Value and lowest E_{lumo} value indicating its brilliant corrosion inhibition properties[67].

The study of the mild steel corrosion inhibition properties of two mercapto-quinoline Schiff bases, 3-((phenylimino)methyl) quinoline-2-thiol (PMQ) and 3-((5-methylthiazol-2-ylimino) methyl) quinoline-2-thiol (MMQT) was done. The results showed that the HOMO orbital geometry of PMQ and MMQT had electron densities that covered the entire structure of the molecules. The two molecules could easily donate electrons to the vacant d-orbitals of the acceptor iron (Fe) found in the mild steel to form coordinate type bonds. PMQ exhibited the highest level of LUMO energy, indicating the superior ability of the molecule to accept electrons [68].

Chapter 3

Methodology

3. Experimental

3.1.1 Materials and reagents

The benzothiophene derivatives were obtained commercially, without prior modifications or purifications. 1 M hydrochloric acid was obtained in the lab with the use of a 37% bench reagent of HCl, which was diluted with distilled water to produce 1 M HCl using the following formulae;

$$C_{(m)} = \left(\frac{\%\times d}{M_r}\right) \times 1000\,, \qquad 3.1$$

$$V_1 = \frac{C_2 \times V_2}{C_1}\,, \qquad 3.2$$

where $C_{(m)}$ represents the concentration in a molar, d is the density, M_r is the molar mass, and V is the volume. Equation 3.1 is used to calculate the concentration of the bench reagent, and equation 3.2 is used to calculate the volume required to prepare 1M concentration. Various concentrations ranging from 100 ppm-500 ppm of the benzothiophene compounds were prepared in an acidic medium. The mild steel working electrode used in the experiment was made-up of a weight percentage (wt%) of 0,46% Mn, 0,26% Si, 0,17% C, 0,019% P, 0,017% S and balance iron (Fe).

3.1.2 Mild steel (working electrode)

A piece of mild steel with the dimensions 1cm×1cm was cut, placed in a Teflon holder, and embedded with an epoxy resin with a $1cm^2$ portion of the surface area left bare. A conducting wire was placed on top of the mild steel sample and held to place using aluminium tape before the epoxy resin solidified. To produce maximum accuracy and precision in the result, the exposed surface of the mild steel was polished with the 200 diameter Struers MD $Piano^{TM}$ 220 mounted on a Struers LaboPOl-1 machine to remove remnants of the epoxy resin on the surface. The surface of mild steel was then polished with SIiC paper with graded grit sizes ranging from 600-1200 to produce a clean, lustrous look on the surface. The surface of the mild steel was then drenched with distilled water, then submerged in acetone, and left to dry in the air prior to any electrochemical experiments. After the surface preparation, the metal alloy was used for Potentiodynamic Polarisation (PDP) and electrochemical impedance spectroscopy (EIS).

3.1.3 Corrosion inhibitors

Various concentrations ranging from 100 ppm-500 ppm of the benzothiophene compounds were purchased from Sigma Aldrich. The stock solution was prepared by diluting 1g with distilled water to produce a solution of 1000 ppm in a 100 mL volumetric flask. The five different concentrations were made in 50 ml volumetric flasks by serial dilution with distilled water in which 10 ml was used as a test solution. The current study used benzothiophene derivatives as corrosion inhibitors for mild steel in 1 M HCl using electrochemical, computational, spectroscopic, and Langmuir methods. The inhibitors were compared based on the different substituents on their ring structure.

The chemical structures and IUPAC names are listed in table 3.1. The effect of the concentration of the inhibitors were studied by testing the various concentrations (100 ppm-500 ppm) in the acidic medium.

Table 3.1 Benzothiophene derivatives chosen for study.

Structure	Name
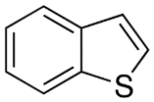	Thianaphthene(B1)
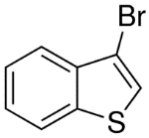	3-Bromothianaphthene(B2)
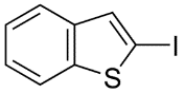	2-Iodobenzothiophene(B3)
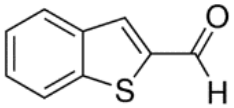	Benzo[*b*]thiophene-2-carboxaldehyde(B4)
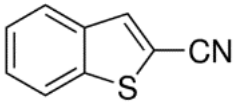	Benzo[*b*]thiophene-2-carbonitrile(B5)

3.2 Methodology

3.2.1 Electrochemical studies

The Auto lab galvanostat/potentiostat (PGSTAT 302N) was used for all the corrosion determinations. An electrochemical set-up of three electrodes, consisting of the following components: mild steel (working electrode), platinum rod, the counter electrode, and the reference electrode composed of Ag/AgCl (in 3 M KCl electrolyte), was used for the experiment. The test solution was exposed to one side of the mild steel electrode, while the surface area (1 cm^2) of the electrode remained constant in the study. The mild steel was subjected to uninterrupted corrosion for 30 minutes before the electrochemical perturbations. A continuous open circuit potential (OCP) was obtained and recorded during the waiting period. Potentiodynamic polarisation (PDP) measurements were determined using the polarisation of the working electrode potential in an interval of -250 mv, and +250 mv while the OCP scan rate was set at 0.001 v/s [69, 70]. The electrochemical impedance spectroscopy (EIS) measurements were conducted using a frequency response analyzer (FRA) module in the auto lab electrochemical machines. Frequency response analyses of the steel/electrolyte interface were recorded at the corrosion potential (E_{corr}) by passing alternating current (AC) through the electrochemical set-up between a 100 000 and 0.1 Hz frequency range, at 0.001 v amplitudes. The experiment was conducted at constant conditions of 303 Kelvin that was maintained using a water bath set at the fixed temperature. PDP and EIS experiments were conducted three times, and the average recorded for analysis.

3.2.2 Spectroscopic studies

A Fourier Transform Infrared (FTIR) spectra of the pure benzothiophene molecules was initially obtained and recorded. The FTIR spectra of the benzothiophene molecules bound on the mild steel surface was also recorded. The process, as mentioned earlier, was done by cleaning and polishing the mild steel sheets and immersing them in 500 ppm of the solution of the inhibitor for seven days. The solution was allowed to be evaporated, and the film of the inhibitor molecule bound on the steel surface was then analysed.

3.2.3 Computational studies

Quantum chemical investigations were done on the neutral molecules of benzothiophene. The density functional theory was employed for the calculations, and the chosen model chemistry used was the B3LYP, 6-31G+ (d, p) functional. The hybrid functional B3LYP was as follows:

$$E_{XC}^{B3LYP}=E_{XC}^{LSDA} + C_1E_X^{B88} + C_2E_C^{LYP} + C_3(E_X^{HF} - E_X^{LSDA}) \quad (3.3)$$

The symbols on the right-hand side of equation 1 represent (from left to right) the local Slater exchange, Vosko, Wilk, and Nussair local correlation, exchange gradient correction of Becke, correction of Lee, Yang, and Parr, exact Hartree-Fock exchange, and the local Slater exchange,

respectively. Chem Office software, Spartan 10. V1.01, was utilised to draw the initial molecular structures. The software was employed for gas-phase geometry optimizations of the molecules. The molecules were minimised to ground state energy, and the process was verified using vibrational frequency calculations, which only produced accurate frequencies of the benzothiophene molecules. Protonation of the benzothiophene molecules was achieved by using the gas phase affinity(PA) values. Computations were carried out in the gas phase on the neutral and protonated entities of the inhibitor molecules and parameters such as highest occupied molecular orbital(E_{HOMO}), lowest unoccupied molecular orbital(E_{Lumo}), energy difference(ΔE), dipole moment(μ), global hardness(η), softness(σ) and electronegativity(χ), were determined. The energy difference(ΔE) is the difference that is obtained when you subtract the energy of the LUMO from that of the HOMO using the following equation:

$$\Delta E = E_{Lumo} - E_{HOMO}. \tag{3.4}$$

The dipole moment is used as an index for the separation of charges(Q) within a molecule and was determined using the following equation:

$$\mu = Q \times r\ , \tag{3.5}$$

where r is denoted as the distance.

Global chemical hardness(η) and softness(σ) reveal more information about a molecule's reactivity. The general principle is that softer molecules are much more reactive than their harder counterparts. This is believed to result from the softer molecules' abilities to receive electrons. The parameters were determined using the following equations:

$$\eta \cong -{}^{1}/_{2}\,(E_{Lumo} - E_{HOMO})\ , \tag{3.6}$$

$$\sigma = -({}^{1}/_{2})(E_{Lumo} + E_{HOMO})\ . \tag{3.7}$$

Electronegativity is known as the tendency of an atom to attract to itself extra electrons and was calculated using the following equation:

$$\chi \cong -({}^{1}/_{2})(E_{Lumo} + E_{HOMO}). \tag{3.8}$$

Chapter 4

Results and discussion

Chapter 4 consists of the results and discussions obtained for electrochemical, quantum chemical, and spectroscopic methods. The methods all have relevant data used in their discussion and analysis. The techniques in this chapter are discussed in the following order: electrochemical methods, quantum chemical methods, spectroscopic methods, and Langmuir isotherms.

The inhibitors in the study were compared based on the substituents attached to the parent ring of benzothiophene (B1). The substituents attached to the benzothiophene ring comprise of bromine (B2), iodine (B3), aldehyde (B4), and carbonitrile (B5).

4.1 Electrochemical studies

4.1.1 Potentiodynamic polarization (PDP)

The reaction of mild steel in an uninhibited (1 M HCl) and inhibited system was investigated using potentiodynamic polarisation techniques. Figure 4.1 shows the PDP curves for benzothiophene inhibitors and their derivatives obtained in the electrochemical study of mild steel in uninhibited and inhibited systems. Through careful observation of the Tafel curves, it is observed that upon introducing the inhibitors to the hydrochloric acid, the anodic and cathodic curves experience a regression in their current density compared to the blank. This observation indicates the inhibitors' abilities to inhibit the hydrogen evolution and mild steel dissolution [71]**.** The lowest anodic currents were observed for the 500 ppm systems for most of the inhibitors in the study. The anodic curves showed significant inhibition, especially at the high concentrations, suggesting the inhibitors successfully adsorbed on the metal surface to form a passive protective film [72]. Figure 4.1 B5 exhibited pseudo-passivation behavior at the anodic branch, most likely due to the compound behaving as a cathodic inhibitor therefore having little to no effect on the anodic reaction [73]. The shape of the anodic Tafel curves remained mostly similar upon the addition of the inhibitors meaning their presence did not alter the reaction mechanism of corrosion. The shape of the cathodic curves remained uniform, except for the B3 and B5 inhibitors, which had a slightly different shape at high concentrations. The uniformity of the cathodic curves suggests that inhibitors B3 and B5 affect the mechanism of the cathodic reaction, which is more evident at higher concentrations [74]. The introduction of the inhibitors led to a decrease in the corrosion potential of all the inhibitors and their respective concentrations. Figure 4.1 B1 shows that introducing the inhibitors at different concentrations leads to a negative shift in their corrosion potential. The negative shift suggests that the inhibitor exhibited cathodic polarization in concentrations 100ppm, 200ppm, 300 ppm, and 500 ppm. The 400 ppm system showed a smaller decrease in the corrosion potential compared to the blank, most likely due to the increase in the anodic reaction and a reduction in the cathodic reaction. Tafel polarization diagrams observed in Figure 4.1 B2, B3, B4 and B5 showed a negative shift in the corrosion potential, almost exhibiting similar trends. There were, of course, exceptions, such as B3 and B4 exhibiting a positive shift in the corrosion potential. An increase in the corrosion potential may be due to a decrease in the anodic reaction due to the formation of a passive film. Figure 4.1 B1 shows that the current density of all inhibited systems is lower than the blank, indicating that all the systems managed to adsorb onto the mild steel surface to limit the corrosion rate. This trend was observed for most inhibitors in the study except for some concentrated systems in Fig 4.1 B3 and B4. This trend can be attributed to the decomposition of the passive film as result of localized corrosion or transpassive reactions such as oxygen evolution [75].

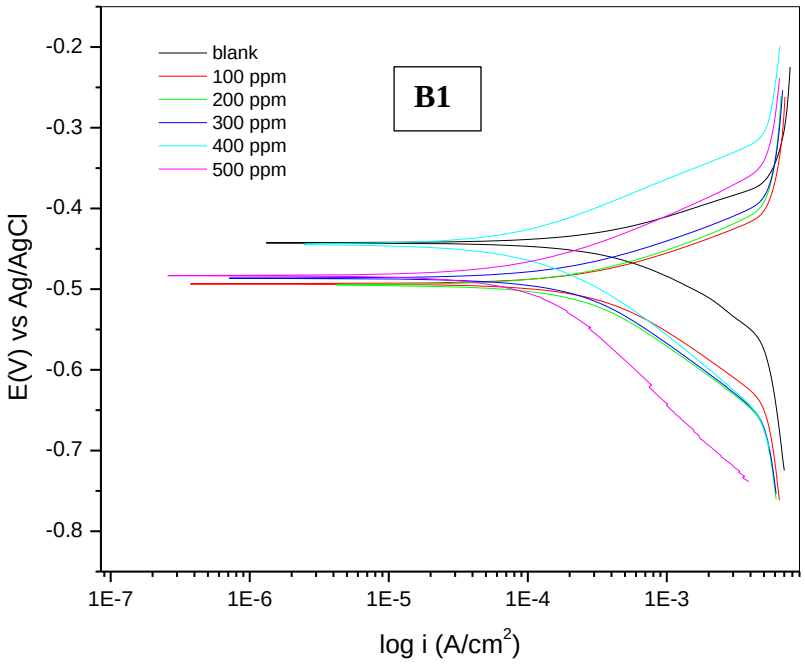
B1
blank
100 ppm
200 ppm
300 ppm
400 ppm
500 ppm
E(V) vs Ag/AgCl
-0.2
-0.3
-0.4
-0.5
-0.6
-0.7
-0.8
1E-7
1E-6
1E-5
1E-4
1E-3
log i (A/cm2)

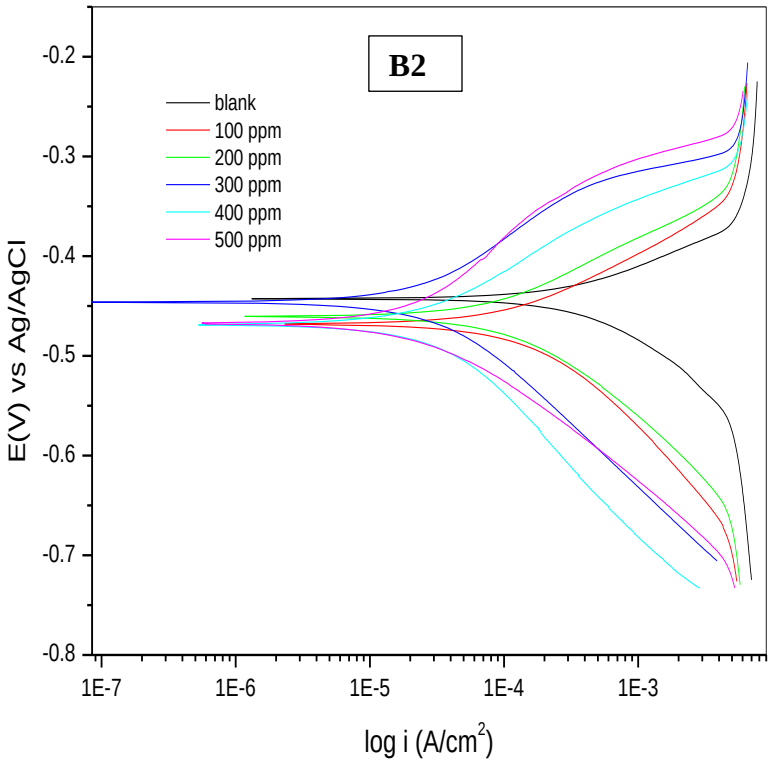
B2
blank
100 ppm
200 ppm
300 ppm
400 ppm
500 ppm
E(V) vs Ag/AgCl
-0.2
-0.3
-0.4
-0.5
-0.6
-0.7
-0.8
1E-7
1E-6
1E-5
1E-4
1E-3
log i (A/cm2)

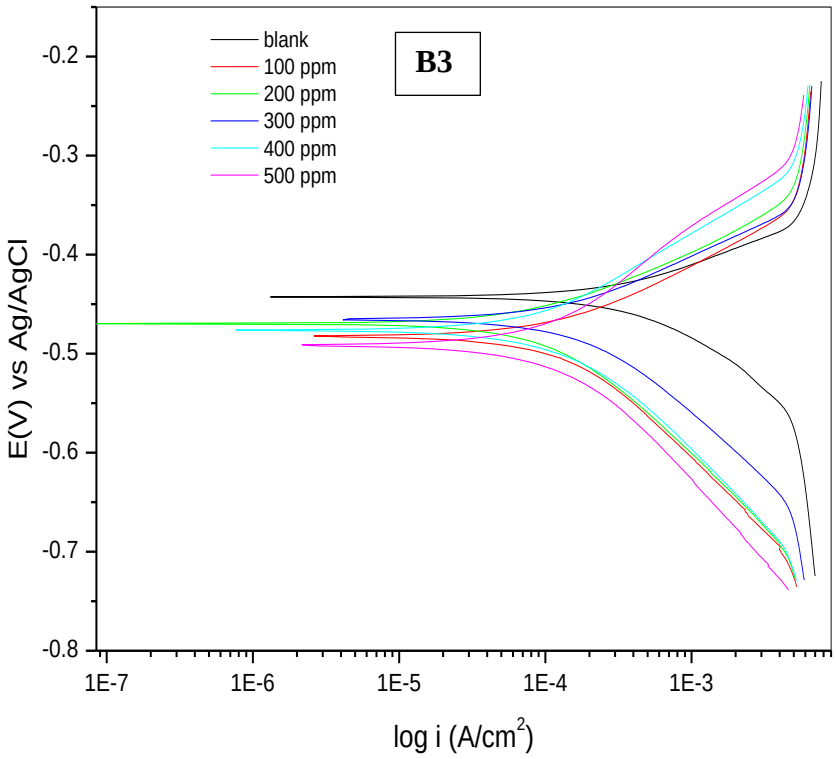
B3
blank
100 ppm
200 ppm
300 ppm
400 ppm
500 ppm
E(V) vs Ag/AgCl
-0.2
-0.3
-0.4
-0.5
-0.6
-0.7
-0.8
1E-7
1E-6
1E-5
1E-4
1E-3
log i (A/cm2)

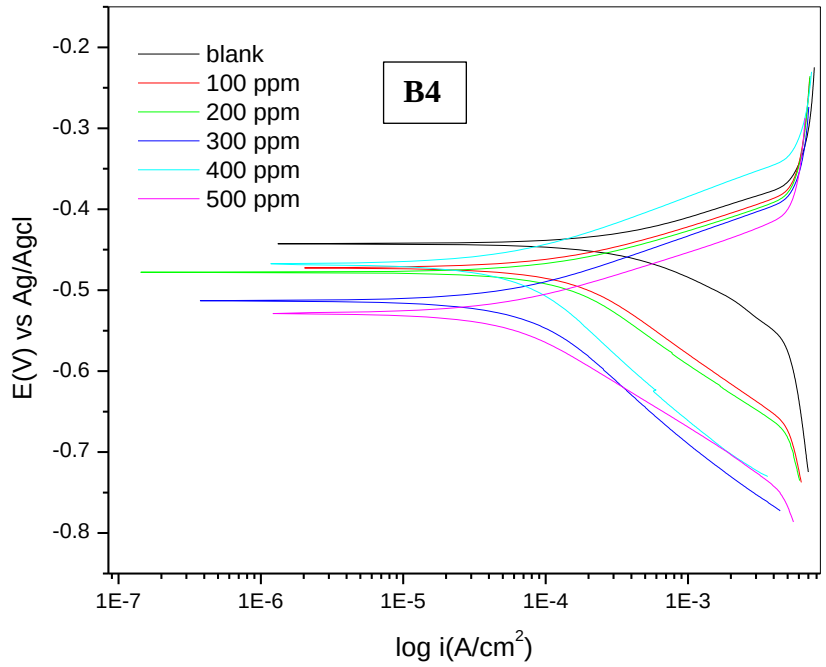
B4
blank
100 ppm
200 ppm
300 ppm
400 ppm
500 ppm
E(V) vs Ag/Agcl
-0.2
-0.3
-0.4
-0.5
-0.6
-0.7
-0.8
1E-7
1E-6
1E-5
1E-4
1E-3
log i(A/cm2)

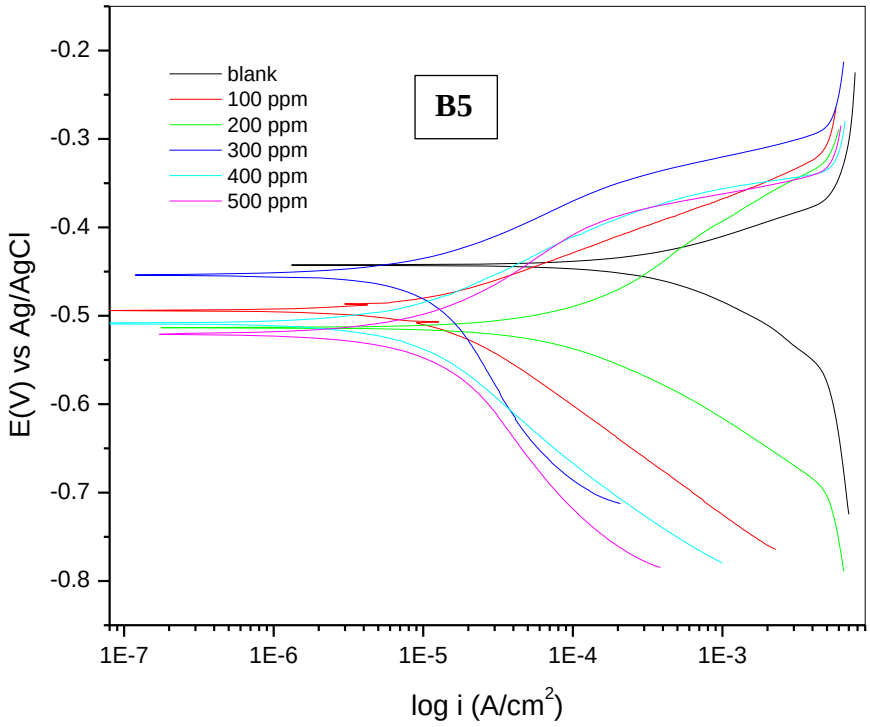

Figure 4.1. Tafel polarization curves for benzothiophene B1, B2, B3, B4 and B5 compounds for mild steel corrosion in 1 M HCl solution.

Table 4.1 shows that the maximum shift in corrosion potential (E_{corr}) of the inhibited systems was mainly observed to be under the standard 85 mv, indicative of mixed-type inhibition. The mixed-type inhibition recorded for most of the inhibitors indicates that the addition of substituents on the benzothiophene rings has no effect on the mechanism of corrosion inhibition for B1, B2, B3, and B5, which have a maximum E_{corr} value shift of 53 mv, 33 mv, 49 mv, and 46 mv, respectively. In contrast, B4 had a maximum difference E_{corr} value of 86 mv, suggesting it was functioning either as an anodic or cathodic type inhibitor. B4 E_{corr} values shifted in a negative direction, inferring that the inhibitor may be acting as a cathodic inhibitor.

The inhibitors and the concentrations influenced the values of b_a and $b_{c,}$ with the effect much more pronounced in $b_{a,}$ indicating a significant increase in the energy barrier for anodic mild steel dissolution in comparison to the cathodic hydrogen proton discharge [76]. The b_c values also indicated a disruption in the cathodic reaction, even if the effects were minimal. Most of the inhibitors functioned as mixed-type inhibitors affecting the metal ionisation and hydrogen evolution reaction, although their anodic reaction was much more noticeable. It is observed that upon the addition of the benzothiophene inhibitors, the current density (i_{corr}) of the reaction experiences a regression, a clear indication of the inhibitor's function in reducing the active sites on the metal surface. The current density values vary from inhibitor to inhibitor, with the substituents in B2, B3, B4, and B5 inhibitors leading to lower current densities than the non-substituted B1 benzothiophene inhibitor. The lower current densities observed for the substituted inhibitors are indicate that the inhibitors' substituents enhance the inhibitors' abilities to eliminate

the active areas on the mild steel surface to limit corrosion. All inhibitors in the study showed appreciable levels of protection efficiency calculated using equation 2.6, with some performing better than others. The inhibition efficiency of the compounds increased when the concentration of the inhibitors was also raised, with the 500 ppm system yielding the highest efficiency among all respective inhibitors in the study. Compared to the non-substituted B1 inhibitor, the substituents in the other inhibitors may be a factor in their superior corrosion protection efficiencies. Observing the inhibition efficiency of all the inhibitors at the highest concentration of 500 ppm, we discern the order of protection efficiency to be B5 > B2 > B3 > B4 > B1. Both B2 and B3 have comparable levels of inhibition efficiency over the investigated concentration interval. The similar protection efficiency values recorded for B2 and B3 made sense as both inhibitors have a halogen substituent on their benzothiophene ring. Halogen-substituted inhibitors are believed to aid corrosion inhibition by dissociating in the corrosion systems and attaching themselves to Fe^{2+} ions on the metal alloy to protect the mild steel from further corrosion and help in adding to the passive film generated by the inhibitors [77-79]. B4 also exhibited a higher protection efficiency than B1. The considerable protection efficiency generated by B4 may result from the pi-electrons in the substituent aldehyde group combined with the pi-electrons present in the benzothiophene ring, allowing B4 to support and enhance donor-acceptor interactions between its molecule and the mild steel surface as opposed to B1. B5 recorded the highest inhibition efficiency compared to other inhibitors in the study. The high protection efficiency of B5 could be attributed to the presence of the carbonitrile group in its ring that provided the inhibitor with additional pi-electrons on top of the pi -electrons present in its benzothiophene ring, which led to better inhibitor-metal interactions. From the results, it can be inferred that adding the substituents in the benzothiophene ring resulted in a better corrosion inhibition efficiency than just the benzothiophene ring functioning as a sole inhibitor.

Table 4.1. Potentiodynamic Polarisation parameters and percentage inhibition efficiencies were obtained from polarisation measurements for the corrosion of mild steel in 1 M HCl with and without different concentrations of the benzothiophene inhibitors.

Inhibitor Concentration (ppm)	$-E_{corr}$ (mV)	β_a ($mVdec^{-1}$)	β_c ($mVdec^{-1}$)	i_{corr} (μAcm^{-2})	$\%IE_{PDP}$ (%)
0	**442**	**73,83**	**54,35**	**255,550**	**-**
		B1			
100	494	144.17	38.38	154.09	39.70%

200	495	41.58	33.42	109.73	57.06%
300	485	34.85	29.05	81.60	68.07%
400	444	120.92	52.75	81.36	68.16%
500	484	84.79	58.69	77.02	69.86%

B2

100	469	68.95	64.99	97.93	61.95%
200	460	65.64	78.52	84.27	67.02%
300	442	137.10	143.28	41.11	84.01%
400	454	141.16	95.19	32.58	87.25%
500	475	87.97	118.87	20.24	92.08%

B3

100	482	117.62	69.43	118.47	53.64%
200	466	117.58	69.74	91.61	64.15%
300	467	33.27	20.92	48.34	81.8%
400	476	41.82	42.68	46.19	81.93%
500	491	27.10	21.79	24.05	90.59%

B4

100	472	124.93	58.89	143.25	43.94%
200	477	127.34	56.28	128.72	49.63%
300	513	167.70	79.15	81.52	68.10%
400	467	168.86	71.21	67.75	73.49%
500	528	113.54	60.07	54.29	78.75%

B5

100	484	124.58	91.89	43.08	83.14%
200	487	126.34	78.22	12.70	95.03%
300	488	119.08	78.22	6.06	97.63%
400	407	39.27	61.52	2.32	99.09%
500	476	101.75	58.22	2.26	99.11%

4.1.2. Electrochemical impedance spectroscopy (EIS)

Electrochemical impedance spectroscopy is an essential technique for characterizing electrochemical systems [80]. EIS measurements analyse the inhibitors' interaction with mild steel in 1 M HCl. The data attained from the Nyquist plots and Bode plots of mild steel, HCl with or without the concentration of the inhibitors, is found in Figure 4.2. The Nyquist plot of the inhibitors depicts a series of depressed semicircles with their respective centres below the x-axis. The diameter of the semicircles exhibits an upward trend when the concentration of the inhibitors is increased. The Nyquist plots display single depressed semicircular properties which are in relation to the single time constant in Bode plots (Fig. 4.3). These properties of the impedance curves suggest that the corrosion of mild steel in the presence of the benzothiophene inhibitors is governed by a single charge transfer process [6]. The depressed semicircles are common among studies involving solid electrodes and usually result from the electrode experiencing frequency dispersion due to the roughness of the electrode surface [81]. The addition of the inhibitors did not change the style of the impedance curves meaning the mechanism of inhibition was similar for all the inhibitors and their concentrated systems. From the curves observed in the Bode plots for the inhibitors in Figure 4.3, the phase angle curves of the Bode plots show the inhibited systems exhibiting a higher area under the curve than the blank system for most of the inhibitors. The inhibitors showing a high area under the curve than the blank implies that most of the inhibitors managed to adsorb on the mild steel surface to form a passive film that shields the mild steel from being exposed to the acid [82, 83]. This held for all inhibitors except B3 and, to a more significant extent, B1, that recorded the lowest inhibition efficiencies values in the PDP and the EIS studies. The low area under curves observed for fig 4.2(a) B1 and (c) B3 suggest that the inhibitors developed a poor passive protective layer on the mild steel to shield it from corrosion in comparison with the other three inhibitors [84].

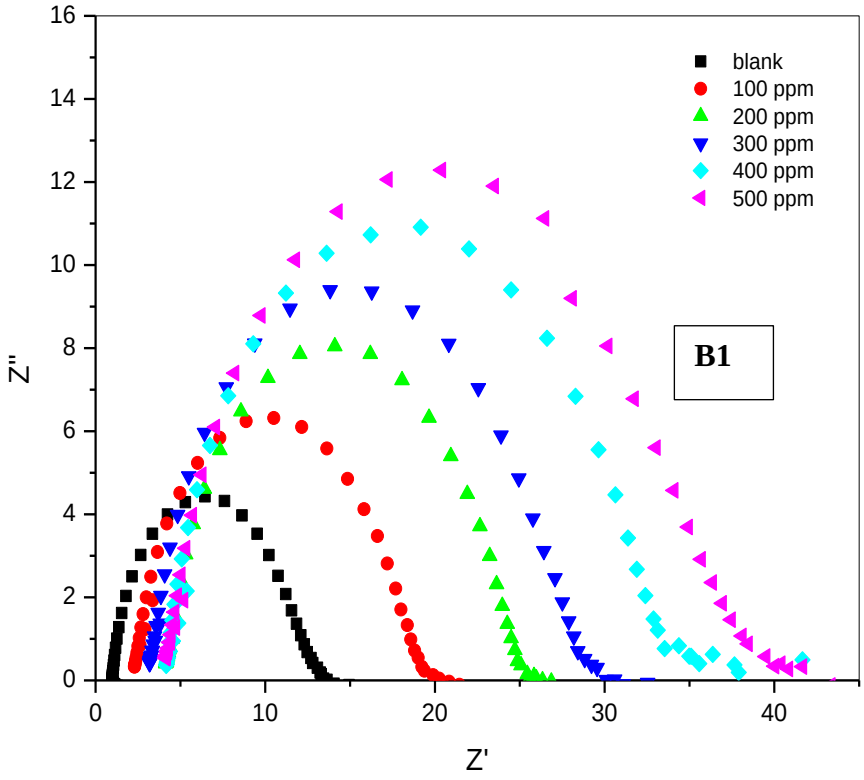
blank
100 ppm
200 ppm
300 ppm
400 ppm
500 ppm
B1
Z''
Z'
0
2
4
6
8
10
12
14
16
0
10
20
30
40

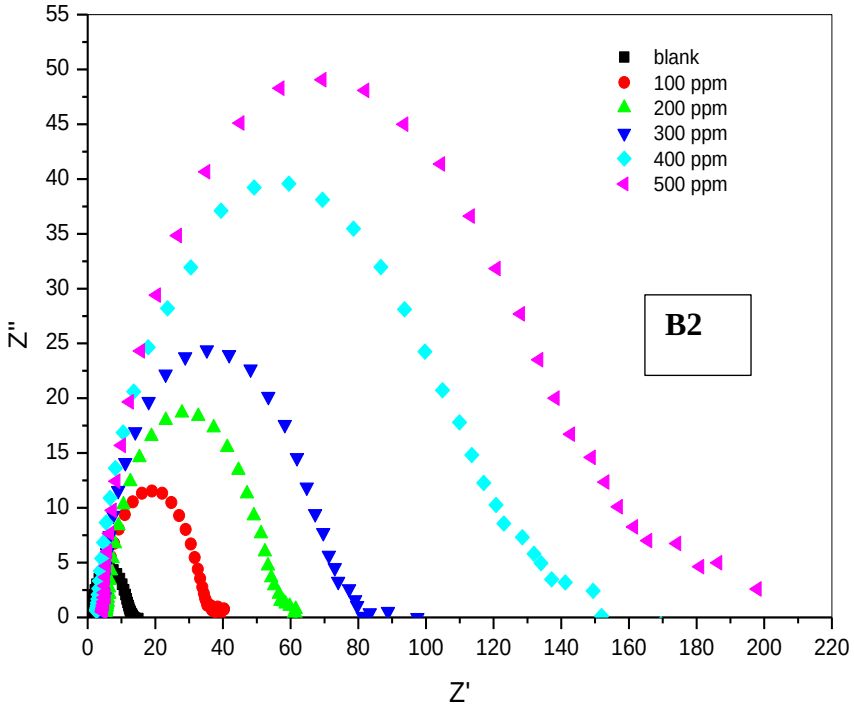
blank
100 ppm
200 ppm
300 ppm
400 ppm
500 ppm
B2
Z''
Z'
0
5
10
15
20
25
30
35
40
45
50
55
0
20
40
60
80
100
120
140
160
180
200
220

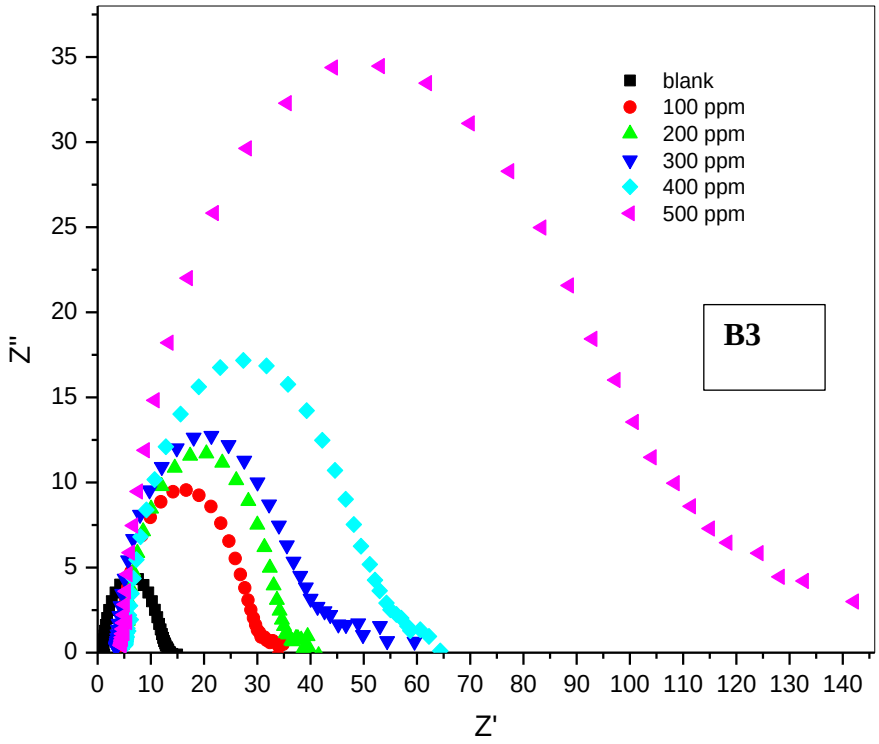
blank
100 ppm
200 ppm
300 ppm
400 ppm
500 ppm
B3
Z''
Z'
0
5
10
15
20
25
30
35
0
10
20
30
40
50
60
70
80
90
100
110
120
130
140

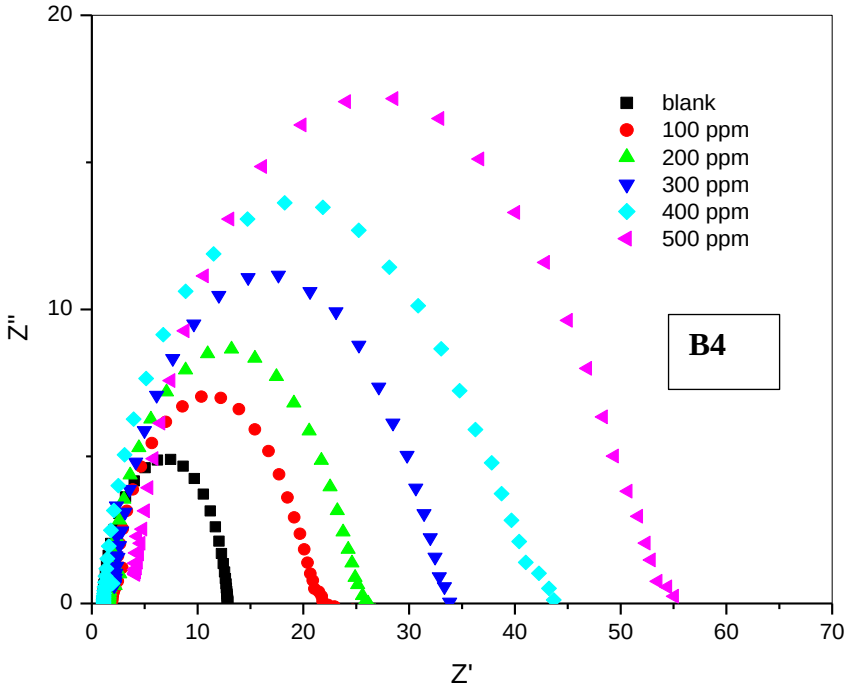
blank
100 ppm
200 ppm
300 ppm
400 ppm
500 ppm
B4
Z''
Z'
0
10
20
0
10
20
30
40
50
60
70

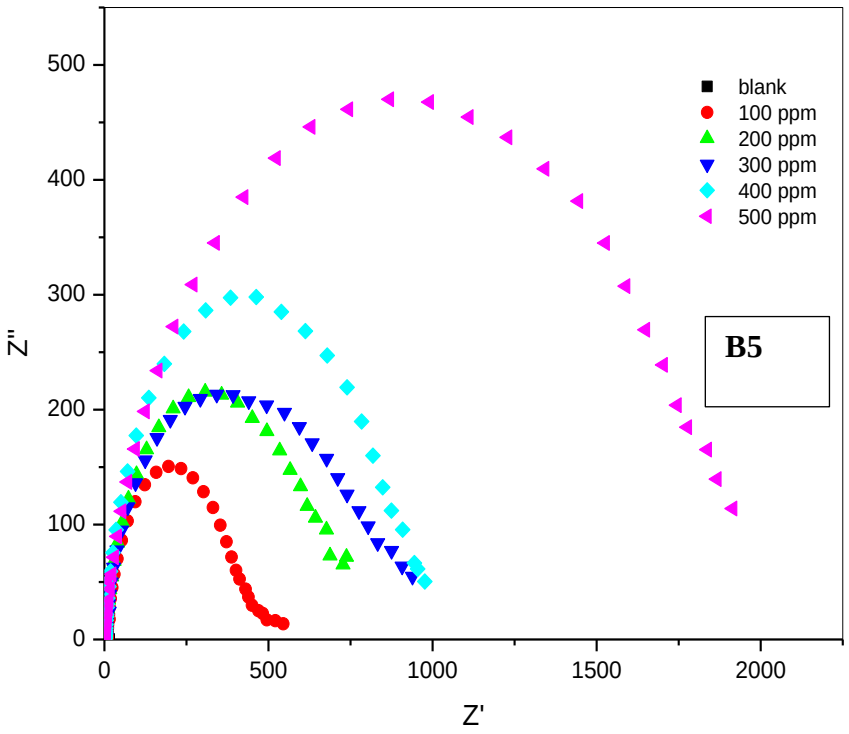

Figure 4.2 Nyquist plot of mild steel in 1 M HCl with and without various concentrations of benzothiophene B1, B2, B3, B4 and B5 inhibitors.

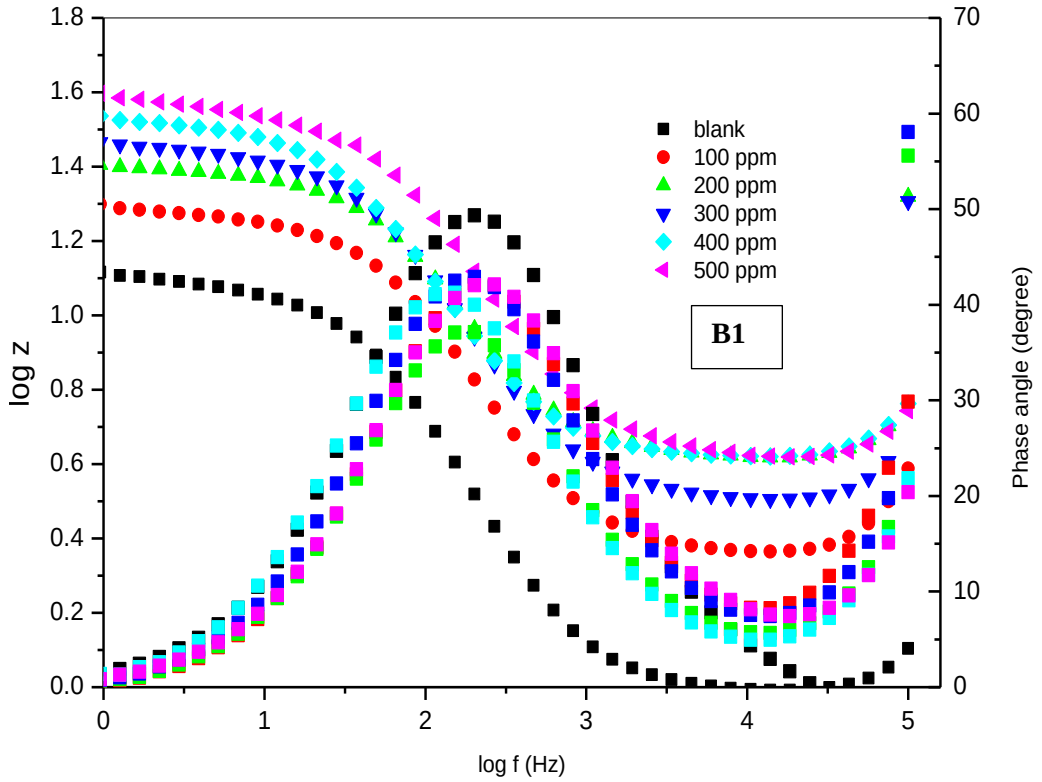
log z
Phase angle (degree)
log f (Hz)
blank
100 ppm
200 ppm
300 ppm
400 ppm
500 ppm
B1

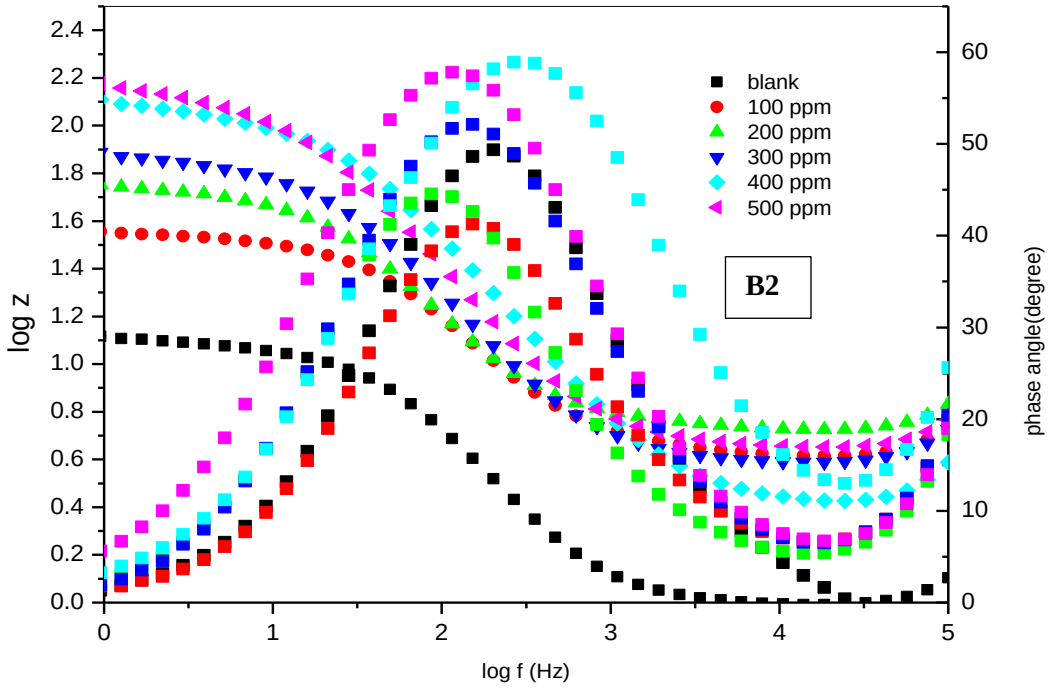
log z
phase angle(degree)
log f (Hz)
blank
100 ppm
200 ppm
300 ppm
400 ppm
500 ppm
B2

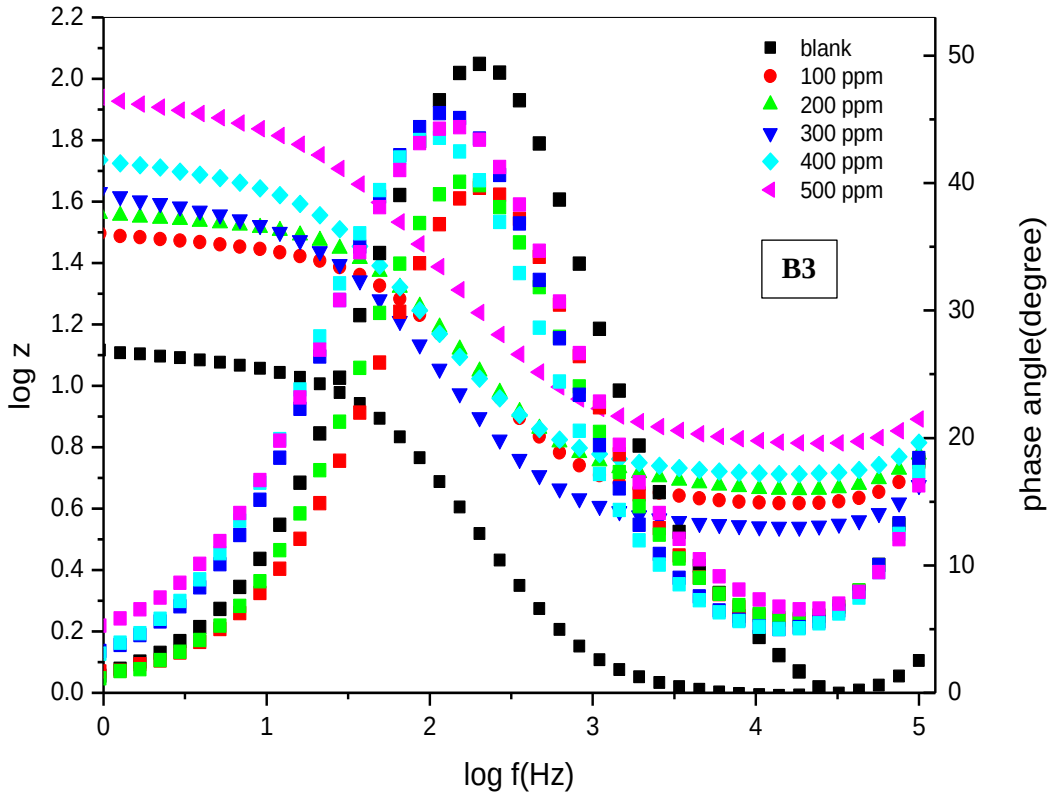
blank
100 ppm
200 ppm
300 ppm
400 ppm
500 ppm
B3
log z
log f(Hz)
phase angle(degree)

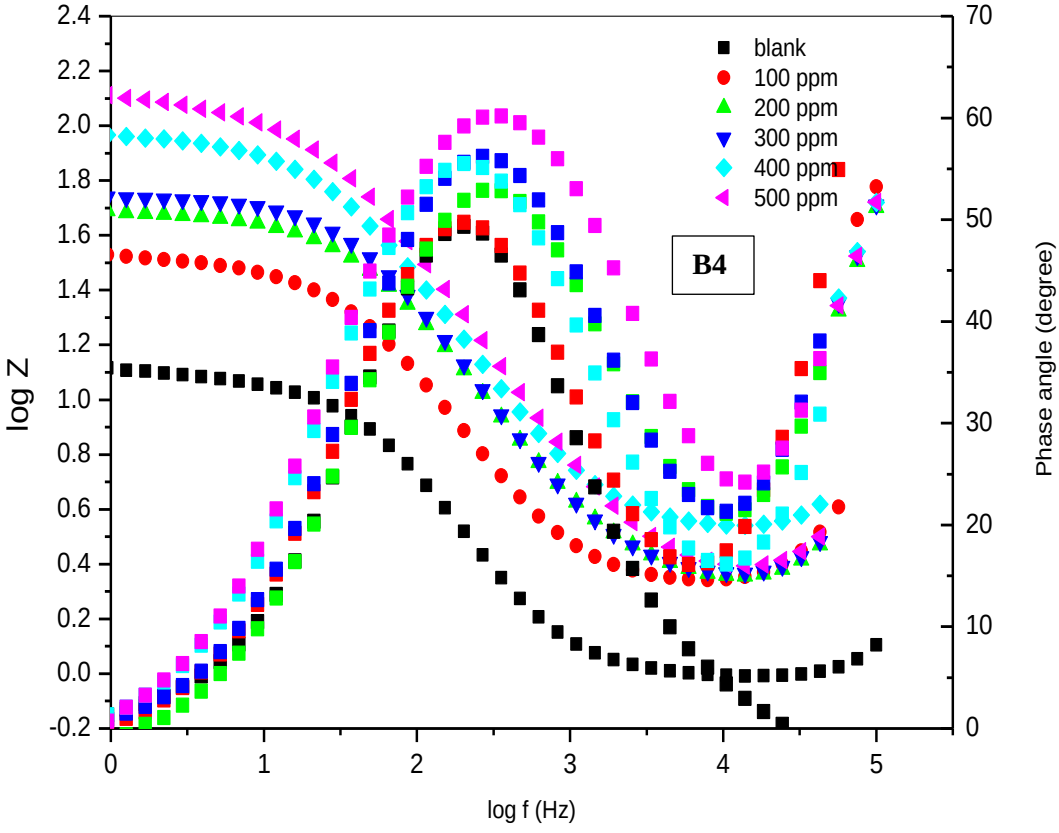
blank
100 ppm
200 ppm
300 ppm
400 ppm
500 ppm
B4
log Z
log f (Hz)
Phase angle (degree)

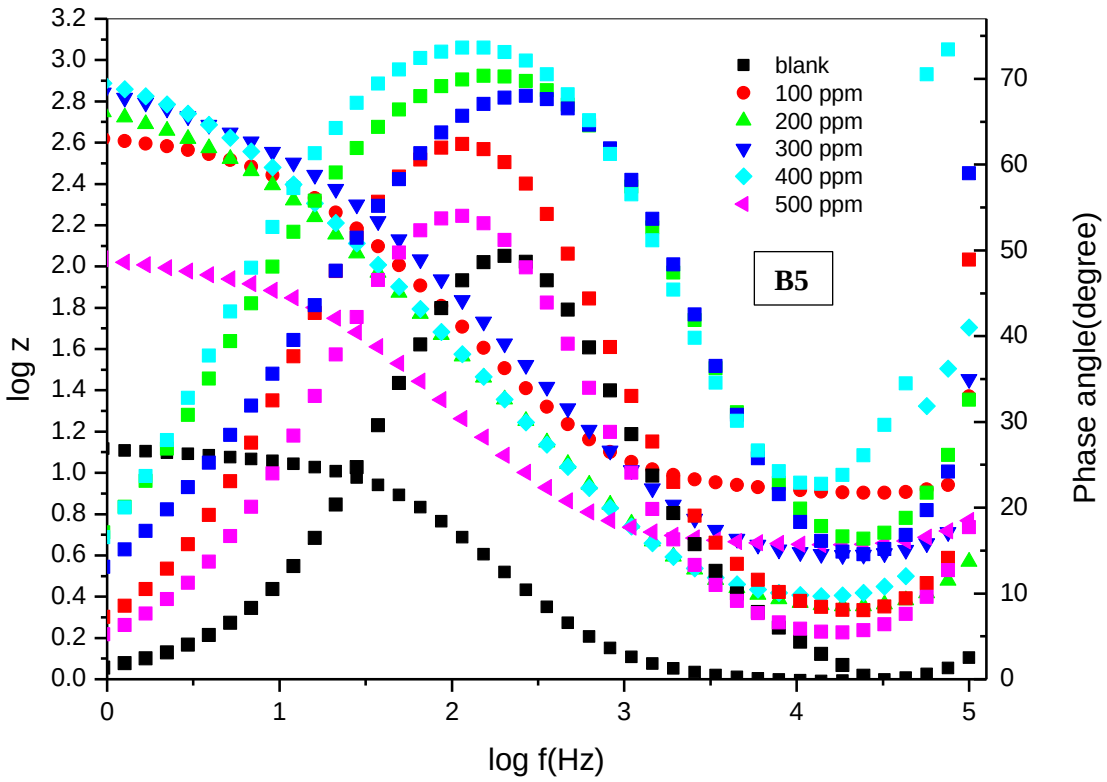

Figure 4.3. Bode plots of mild steel in 1 M HCl with and without various concentrations of benzothiophene B1, B2, B3, B4 and B5 inhibitors.

Table 4.2 shows the impedance parameters of the study, such as the charge transfer resistance (R_{ct}), solution resistance (R_s), and gauge inhomogeneity (n) attained after fitting the Nyquist plots. Parameters such as the double-layer capacitance (C_{dl}) and inhibition efficiency ($IE_{EIS}\%$) were determined using equations (3.3) and (2.1), respectively. Table 4.2 shows that the benzothiophene inhibitors recorded a higher solution resistance than the value observed for the blank. This result is an indication of the inhibitors' ability to decrease the conductivity of the solution. In addition to exhibiting a higher solution resistance than the blank, the benzothiophene substituted compounds also had better R_s values than the non-substituted compound. The presence of the substituents led to an increase in the ability of the inhibitors to decrease the conductivity of the corrosion solution system. The next trend of interest was the constant phase potential (CPE). The CPE constant (Q) values of the uninhibited system were significantly higher than those of the inhibited systems of the benzothiophene inhibitors. This could result from the cover or film the inhibitors produced on the mild steel surface. The film protected the surface area of the mild steel from ions that could lead to its eventual corrosion. The inhibited systems exhibited lower or equal values of the CPE exponent (n) compared to the uninhibited systems for all inhibitors, with B4 being the only exception. The lower CPE exponent (n) indicates the absorption of the benzothiophene inhibitors

on the mild steel surface because of the increase in the inhomogeneity of the surface of the mild steel electrode in the inhibited systems [85].

The R_{ct} values of the inhibited systems were much larger than the uninhibited systems. They were observed to be increasing with the concentration, most likely due to the ability of the inhibitors to disrupt the movement of the charges in the electrochemical systems. The high R_{ct} values of the inhibited systems also coincided with an increase in the protection efficiencies (IE_{EIS}) of the inhibitors. The trend of all the inhibitors' maximum concentration (500 ppm) protection efficiencies (IE_{EIS}) agrees with the order determined for polarization studies, the protection efficiencies using equation 2.6 . The double-layer capacitance (C_{dl}) values for most of the inhibitors were lower than the C_{dl} values of the uninhibited system; however, there were exceptions for B2 100 ppm, B3 300 ppm and 400 ppm, and the entire B5 inhibitor. The low values of the inhibited system could be attributed to a low dielectric constant in the system or a reduction in the area of the electrode exposed to corrosive ions and an increase in the depth of the protective film [86]. At the same time, the observed C_{dl} values were higher than the blank and could be attributed to the increase in the dielectric constant. This suggests that the passive film may have absorbed additional water during the reactions[87].

Table 4.2. Electrochemical impedance spectroscopy parameters and percentage inhibition efficiency for corrosion of mild steel in 1 M HCl containing different concentrations of benzothiophenes inhibitors.

Inhibitor Concentration (ppm)	Rs (Ωcm^2)	Q, Yo (F)	n	R_{ct} (Ωcm^2)	C_{dl} ($\mu F \cdot cm^2$)	$\%IE_{Eis}$ (%)
0	1.00	618	0.88	11.9	208	-
			B1			
100	2.33	395	0.85	17.4	187	31.61%
200	4.19	308	0.85	21.2	139	43.87%
300	3.21	322	0.84	26.1	180	54.41%
400	4.22	333	0.85	30.4	165	60.86%
500	4.15	239	0.82	35.0	175	69.86%
			B2			
100	4.17	320	0.82	32.3	233	63.16%

200	5.42	315	0.84	51.9	208	77.07%
300	3.89	224	0.84	73.7	135	83.85%
400	2.56	140	0.83	126	109	90.55%
500	4.47	173	0.85	150	111	92.08%
			B3			
100	4.15	281	0.83	27.0	166	55.93%
200	4.65	276	0.84	31.9	166	62.70%
300	3.48	453	0.82	40.1	401	70.32%
400	5.18	351	0.82	50.2	296	76.29%
500	4.47	241	0.84	109	177	88.98%
			B4			
100	1.79	192	0.99	18.76	208	39.45%
200	1.39	178	0.99	23.15	194	50.93%
300	1.64	130	0.99	31.17	141	63.55%
400	0.51	126	0.99	39.97	137	71.58%
500	3.62	62.7	0.99	47.88	67.9	76.27%
			B5			
100	4.23	79.4	0.73	164	259	92.74%
200	4.02	82.5	0.84	343	581	95.03%
300	8.01	70.6	0.86	433	379	96.53%
400	3.64	64.1	0.84	733	497	98.38%
500	2.24	83.5	0.88	862	384	98.62%

4.2 Computational studies

The inhibitor molecules were optimised to ground state minimum energy, and the structures are shown in Figure 4.4. This minimum potential energy's validity was confirmed using vibrational frequency calculations, producing only accurate frequencies. The optimised geometry structures of the compounds were of particular importance. The geometry structure is closely associated with its efficacy as a corrosion inhibitor. Planar geometrical inhibitors show better corrosion inhibition than less planar geometry compounds[88, 89]. The planar geometrical configuration enables the inhibitor molecules to cover a large surface area of the mild steel surface, a trait reported less in non-planar geometrical structures. Molecules that are planar geometrically can also present the most, or all, atoms in their arsenal to come into contact with metal surfaces, which is a desirable trait in corrosion inhibition. Benzothiophene has a planar geometry, and so have the rest of the studied inhibitors. The structure of the compound is equipped for corrosion inhibition, and a thorough investigation into its quantum chemical parameters revealed its corrosion inhibition performance.

B1

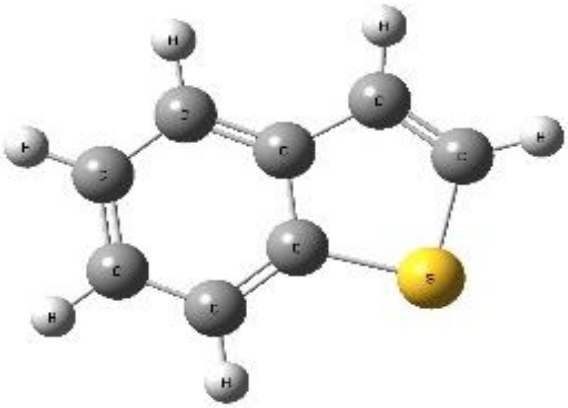

B2

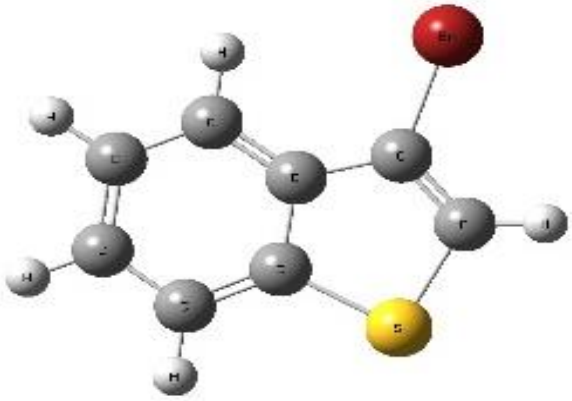

B3

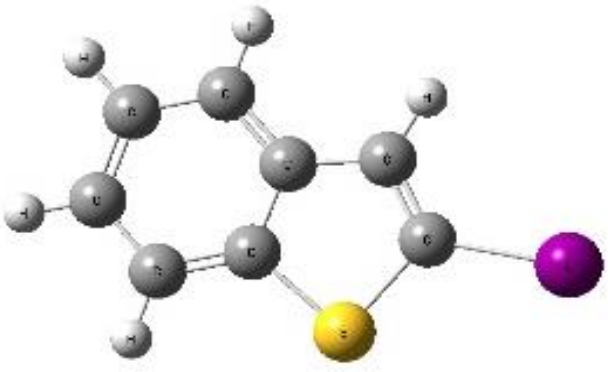

B4

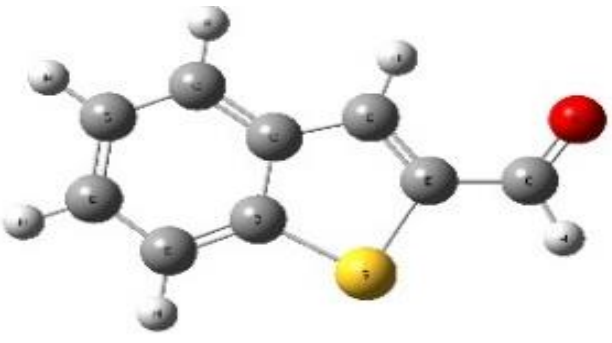

B5

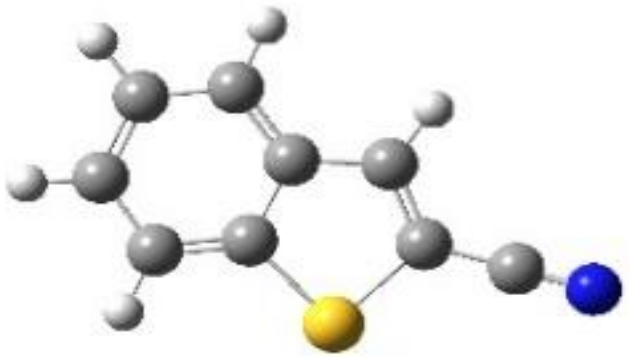

Figure 4.4. Optimised structure of benzothiophene molecules: carbon (grey); hydrogen (white); sulphur(yellow) ; bromine (red) and iodine (purple); oxygen (red) and nitrogen (blue).

Figure 4.5 below consists of the electron density graphics of the highest occupied molecular orbital (HOMO) and the lowest unoccupied molecular orbital (LUMO) of the optimised structures of the benzothiophene inhibitors. The HOMO orbital of the inhibitors is mainly distributed over their entire rings, suggesting that the molecules are active sites for electrophilic attack by the metallic cations. The molecules exhibited a pi-character delocalised over most of the compounds' atomic rings. The delocalised HOMO electron densities favour the forward donation of the electrons to the vacant d-orbitals of the Fe (mild steel) during the donor-acceptor interactions. From the HOMO structure of the inhibitors, it was observed that the entire aromatic structures were involved in the forward donation of electrons to Fe in mild steel. The Homo orbitals of benzothiophene derivatives were able to exhibit forward donation likely due to the widely delocalised electron density of the inhibitors corresponding to the excellent inhibition efficiency of the molecules.

From Figure 4.5, it is observed that the LUMO diagrams for most of the inhibitors are similar, with the electron density distributed over their entire structural rings. The high LUMO elecctron density observed for the inhibitors is an indication of the molecules' excellent disposition to accept

electrons from the metals in back-donation interactions. The only exception was the LUMO of B3, which is distributed mainly to the thiophene ring and iodine atom, suggesting an ability of the iodine atom to accept electrons.

HOMO

B1

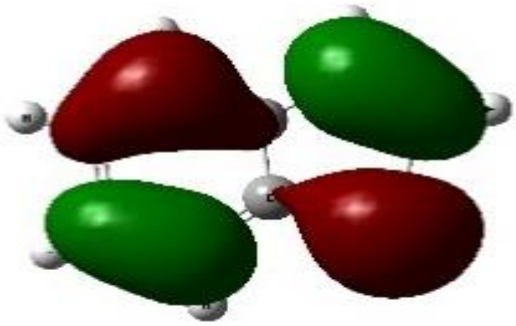

B2

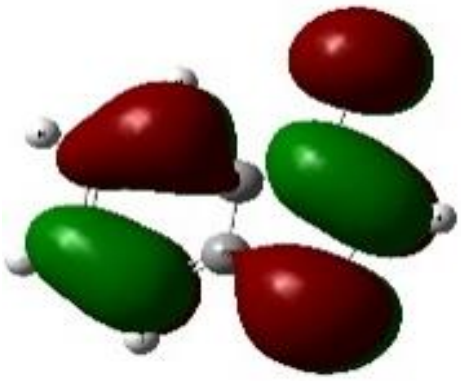

B4

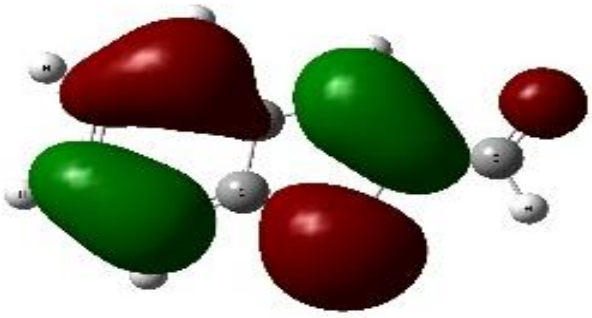

B3

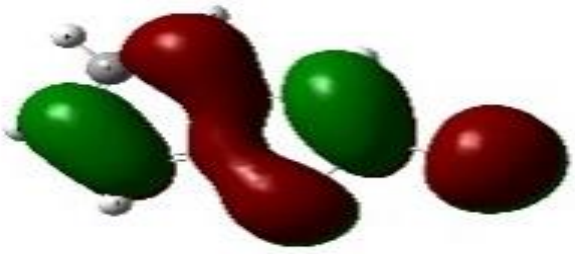

B5

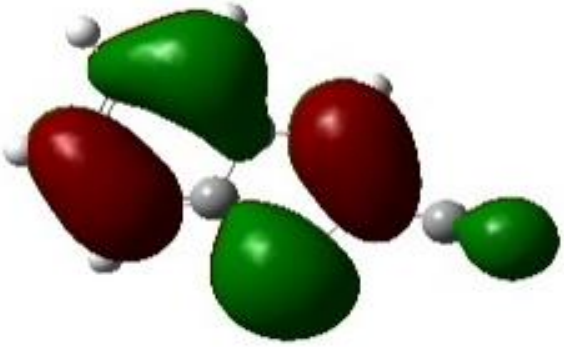

LUMO

B1

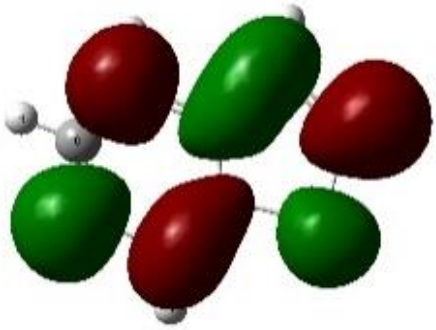

B2

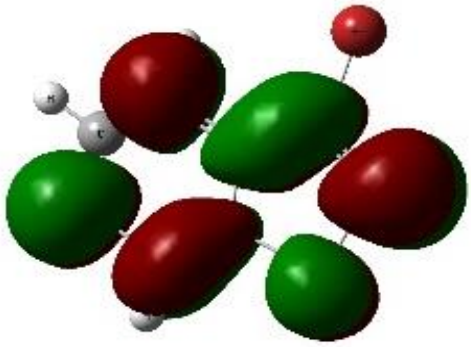

B4

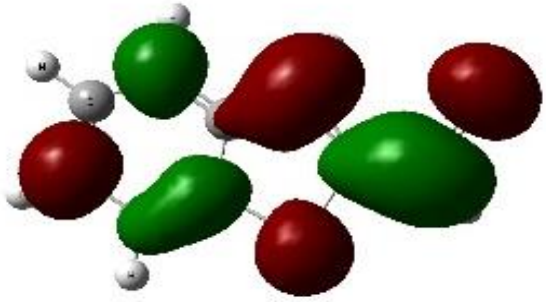

B3

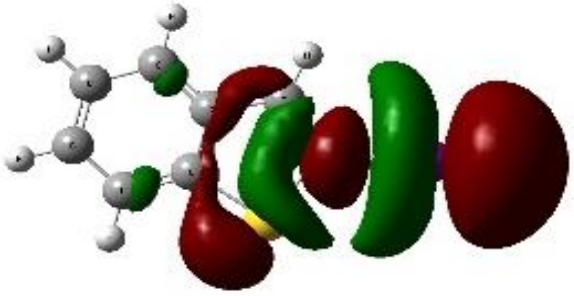

B5

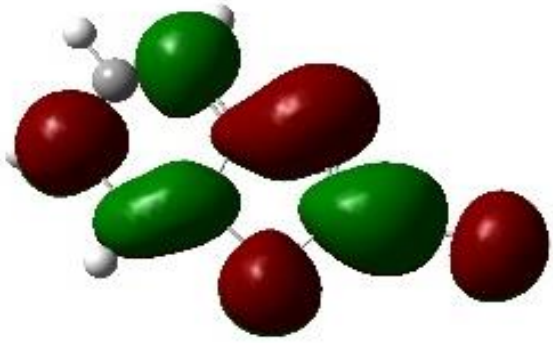

Figure 4.5 Electron density isosurfaces of the HOMO (top) and the LUMO (bottom) of the studied benzothiophene inhibitors.

Table 4.3 shows the HOMO energy (E_{HOMO}) associated with the molecule's ionisation energy, accentuating how a molecule can accept electrons from donating species. The order of decreasing E_{HOMO} is B1 > B3 > B2 > B4 > B5. This trend does not agree with the order of the protection efficiencies observed in the electrochemical study. In this trend, B1 has the highest electron-donating ability. The high E_{HOMO} of B1 may be due to the absence of highly electronegative atoms like bromine, iodine, nitrogen, and oxygen, leading to lower electronegativity, as shown in Table 4.3. The opposite holds for a molecule's LUMO energy (E_{LUMO}) associated with its electron affinity. The decreasing order of E_{LUMO} is B1 > B2 > B3 > B5 > B4. A lower LUMO energy means a molecule can easily accept electrons from the metal atom. The trend is not aligned with the experimental inhibition efficiencies, which suggests that the inhibition potentials of the inhibitors are not entirely informed by their ability to receive electrons from the occupied orbitals of Fe [90]. However, Table 4.3 shows that B1 is less prone to accepting electrons from the metal during back-donation than the substituted benzothiophene inhibitors. The low E_{LUMO} recorded for B1, indicates that the substituents encouraged the propensity of the benzothiophene ring to accept electrons from the mild steel. The frontier orbital theory shows that an inhibitor's adsorption to metal is governed by the energy difference between the HOMO and LUMO, an entity known as the energy gap. A smaller energy gap is desired because it means the ability of a molecule to donate and accept electrons is enhanced [91]. The decreasing order of the energy gap is B1 > B2 > B3 > B5 > B4. B4 had the lowest reported energy gap in the study. However the difference in the energy gap values were not significant, indicating that the inhibitors exhibit high levels of reactivity. In addition to the HOMO, and LUMO and their energies, a helpful parameter in investigating corrosion performance is the dipole moment (μ) [92]. The dipole moment is obtained from the density functional theory calculations with larger positive values for molecules considered as good corrosion performance [93]. From the table, values of μ follow the trend of B5 > B4 > B3 > B2 > B1. B1 is recorded to have the lowest dipole moment. The low dipole moment for B1 was a consequence of the stronger polarity of the C-I, C-Br, C-O, and C≡ N bonds in B3, B2, B4, and B5, respectively. Global hardness (n) and electronegativity (χ) are additional quantum chemical parameters used to probe into an inhibitor's corrosion performance. The parameters are determined using equations 3.6 and 3.8, respectively. Softer (low n) molecules are considered much more reactive than their rigid counterparts. The decreasing order of global hardness was determined to be B1 > B2 > B3 > B5 > B4, which showed that B1 was the hardest molecule in the study. The global hardness value of B1, shows that the presence of the substituents in the other inhibitors led to an increase in their reactivity and inhibition potential. The electronegativity results in Table 4.3 showed B1 as the least electronegative in the study. The low electronegativity of B1 was expected, as the inhibitor did not have an electronegative atom attached to its benzothiophene ring. The decreasing order of electronegativity was determined to be B4 > B5 > B2 > B3 > B1. Inhibitors with low electronegativity values are favored in corrosion protection because they can donate electrons unlike highly electronegative molecules [94]. B4 showed the highest electronegativity due to the electronegative aldehyde group in the benzothiophene group. B5 also had a reasonably high electronegativity due to the electronegative carbonitrile group, similar to the presence of

halogens in B2 and B3. The substituents in B5, B4, B3, and B2 increase the propensity of the molecules to donate electrons to vacant d-orbitals in the mild steel.

Table 4.3. Quantum chemical parameters for the studied benzothiophene inhibitors.

Inhibitor molecule	E_{HOMO} (eV)	E_{LUMO} (eV)	ΔE (eV)	μ (D)	η (eV)	χ (eV)
B1	-6.24	-1.08	5.16	1.06	2.58	3.66
B2	-6.41	-1.39	5.02	1.28	2.51	3.9
B3	-6.29	-1.41	4.88	1.53	2.44	3.85
B4	-6.72	-2.69	4.04	4.25	2.02	4.71
B5	-6.85	-2.29	4.56	5.51	2.28	4.57

4.3 Spectroscopic studies

4.3.1 Fourier transform infrared spectrometer (FTIR)

The spectral for the pure benzothiophene inhibitors and the adsorbed film of the benzothiophene inhibitors on the mild steel surface of the inhibitors after seven days of immersion in 500 ppm benzothiophene in 1 M HCl, is presented in Figure 4.6. Figure 4.6 shows the varying chemical interactions of the functional groups of the benzothiophene inhibitors. From the pure spectra of the inhibitors, the characteristic C-H vibrational bands are located at 3050 cm^{-1}. At the same time, the characteristic aromatic peak was observed at 1450 cm^{-1}. The peak observed at 690 cm^{-1} - 990 cm^{-1} resulted from the distinct C-H bond that bends out of the plane [95]. Characteristic aromatic stretching C-C frequencies were observed above 1500 cm^{-1}. In the pure spectra of B2, the strong peak around 620 cm^{-1} is believed to be the C-I vibrational band, while for B3, the strong peak found in the range of 550 cm^{-1} – 700 cm^{-1} could be attributed to the vibrational band for C-Br [96]. Carbonyl (C=O) stretching vibrational bands for B4 are identified at a frequency of about 1600 cm^{-1}. The strong peak above 2000 cm^{-1} for B5 was identified as a C≡ N stretching vibrational band.

Through careful observation of the benzothiophene inhibitors' adsorbed film spectra, it appears that the bands in the region of 490 cm^{-1}-2000 cm^{-1} have disappeared for all the inhibitors compared to their pure spectra. In the range of these stretching frequencies, it can be implied that the halogen substituent in B2 and B3, along with C≡ N in B5, were actively involved in the inhibitors' interaction with the mild steel [97]. The aromatic C-C stretching bands underwent a slight frequency shift in the spectral of the adsorbed film of the inhibitors, and it can be implied that they might have interacted with the mild steel surface. The large and broad peak observed

between 3100 cm^{-1} and 3500 cm^{-1} reported for the spectra of the adsorbed film was identified as the hydroxyl group and is written for all inhibitors in the study. This particular peak was not observed for the inhibitors' pure spectra, suggesting that new bonds were formed in the inhibitor-mild steel complex [98].

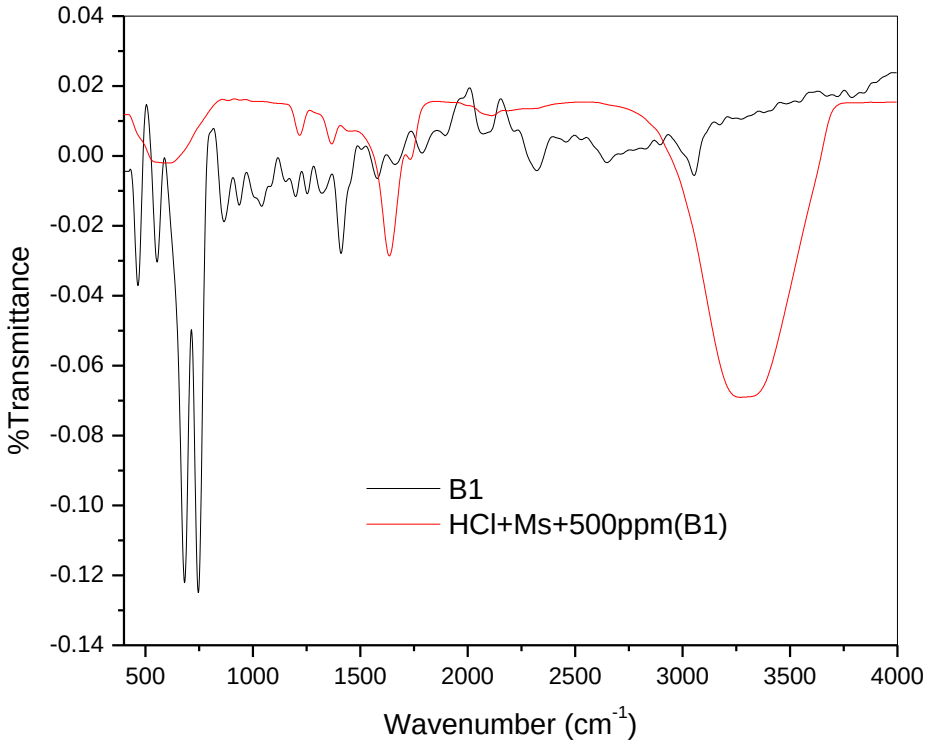

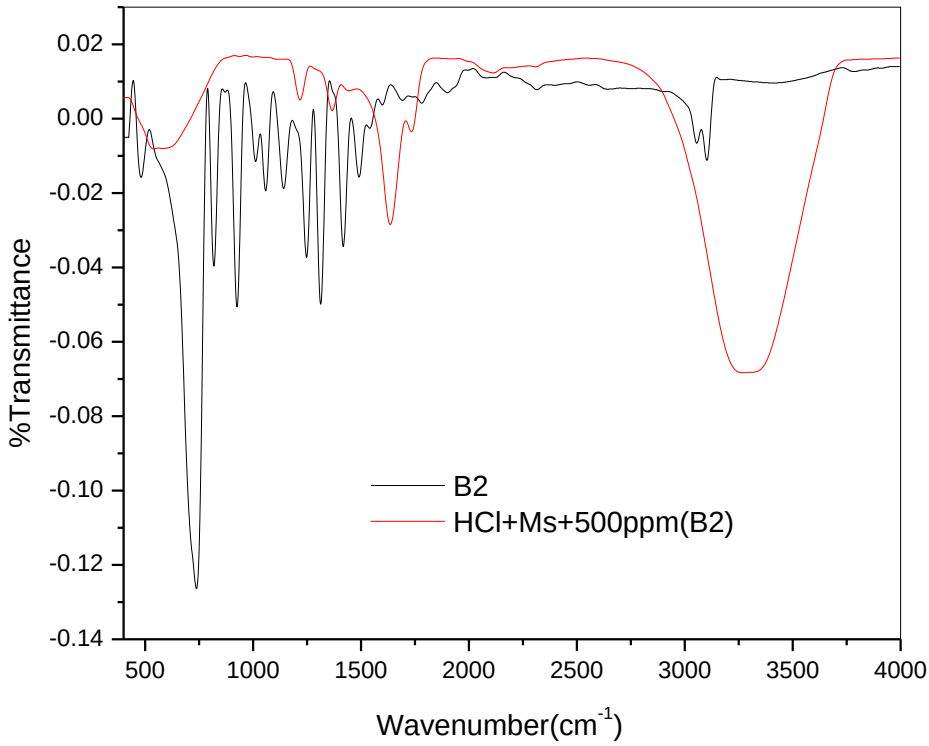

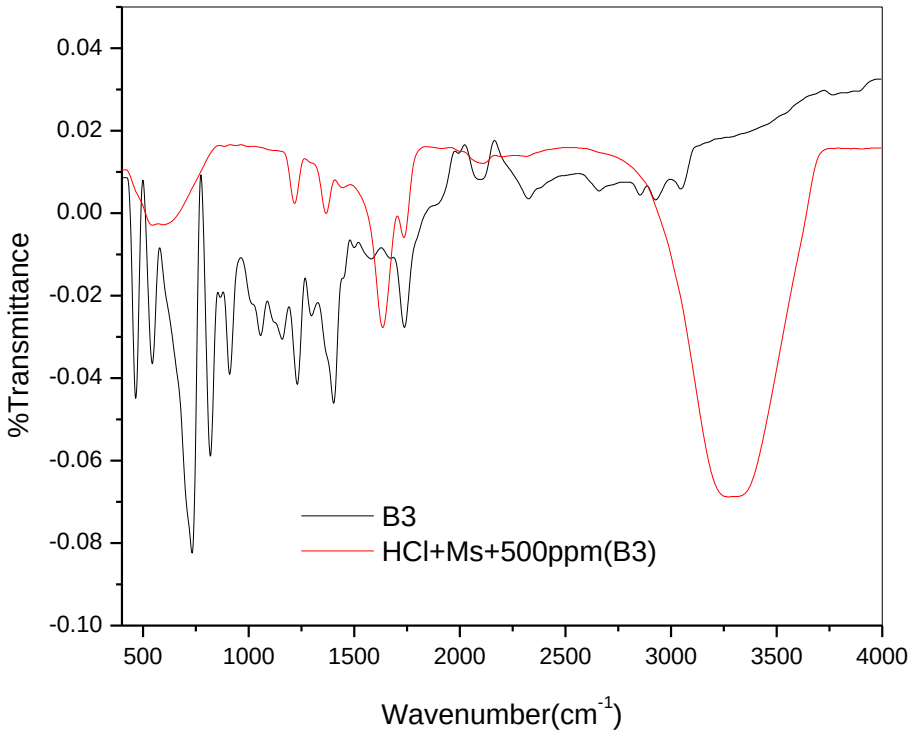
0.04
0.02
0.00
-0.02
-0.04
-0.06
-0.08
-0.10
%Transmittance
500
1000
1500
2000
2500
3000
3500
4000
Wavenumber(cm-1)
B3
HCl+Ms+500ppm(B3)

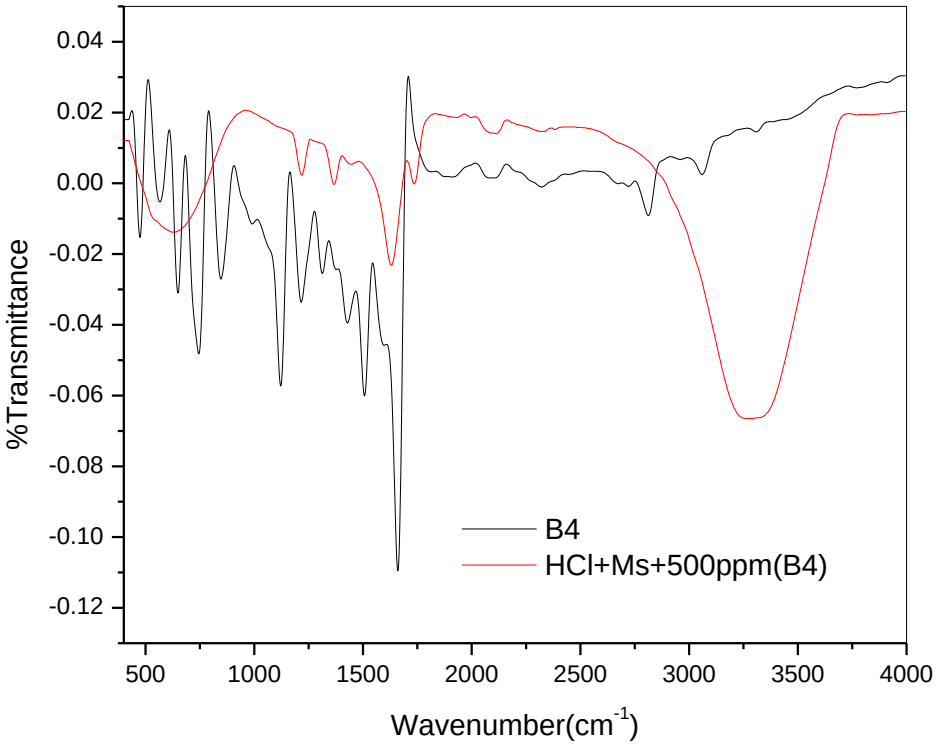
0.04
0.02
0.00
-0.02
-0.04
-0.06
-0.08
-0.10
-0.12
%Transmittance
500
1000
1500
2000
2500
3000
3500
4000
Wavenumber(cm-1)
B4
HCl+Ms+500ppm(B4)

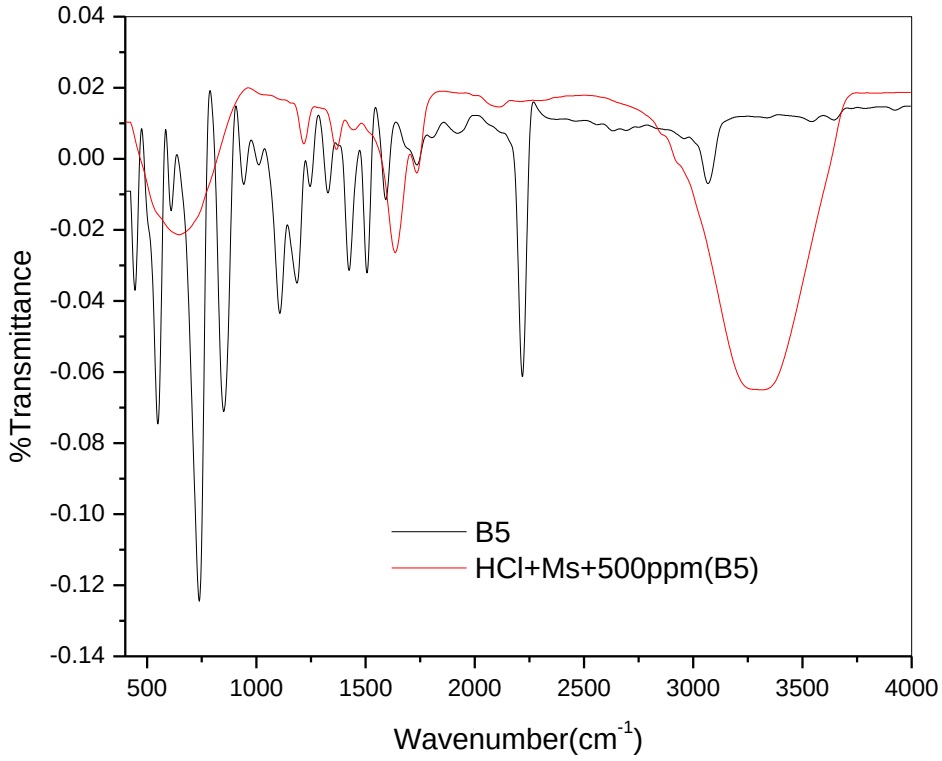

Figure 4.6. FTIR spectra of the studied pure benzothiophene inhibitor molecules and their adsorbed film on a mild steel surface after seven days' immersion in inhibitor-acid solutions.

4.4 Langmuir adsorption isotherm

Figure 4.7 shows the EIS plots of the Langmuir isotherms for mild steel in 1 M HCl in the solution of the studied benzothiophene inhibitors. The isotherm shows an appreciable linearity level, implying the conformity to experimental data. Through careful observation of the slopes of the studied benzothiophene inhibitors, it is shown that they are close to unity for the Langmuir isotherms. The slight deviations resulted from the reactions that occurred in the adsorption layer [99].

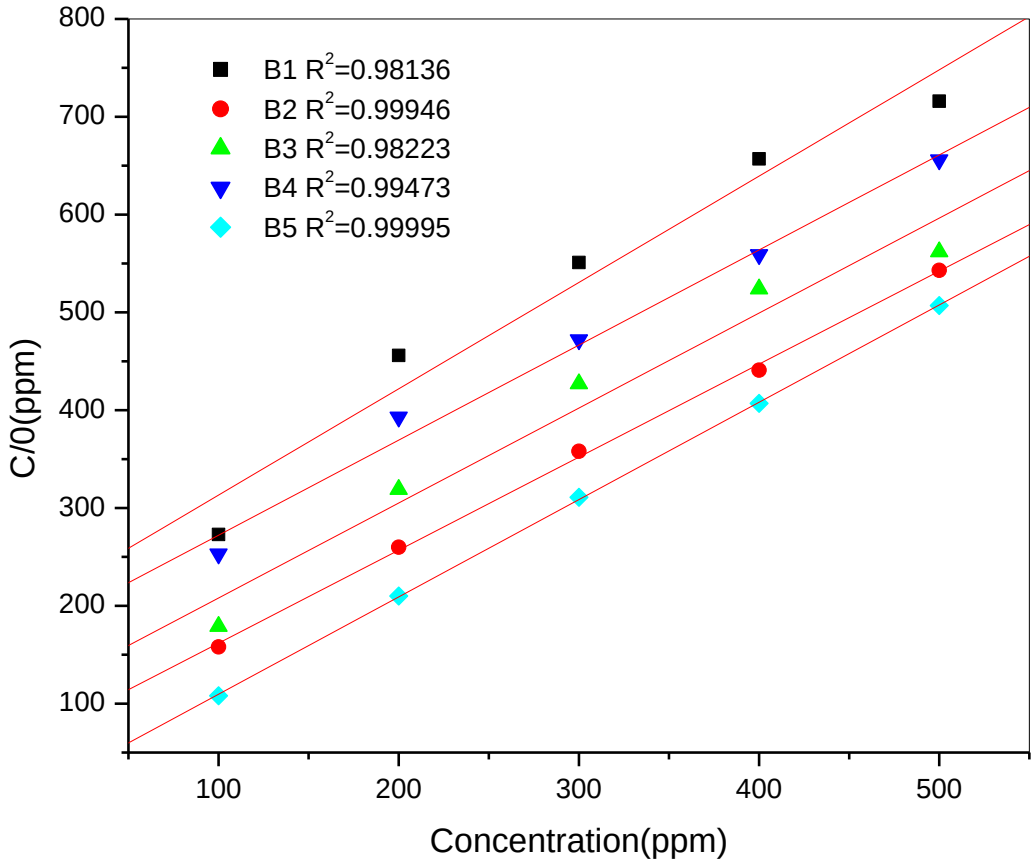

Figure 4.7 Langmuir adsorption theorems plot for B1, B2, B3, B4, and B5 using EIS experimental data**.**

Table 4.4 shows the values of the equilibrium constant of the adsorption/desorption (K_{ads}) and Gibbs free energy (ΔG°_{ads}). The benzothiophene inhibitors produced negative values of ΔG°_{ads} and large values of K_{ads} suggesting that the adsorption of the benzothiophene inhibitors on the mild steel surface was strong and spontaneous. The mode of adsorption of the inhibitors was discerned by examining the magnitude of the Gibbs free energy (ΔG°_{ads}). When the values of Gibbs free energy are in the range of -20 $kJ\ mol^{-1}$, it is usually indicative of a physical adsorption process. A value of the Gibbs free energy around - 40 $kJ\ mol^{-1}$ signifies a chemical adsorption process. A value between the two figures indicates a mixed-type form of adsorption. From Table 4.4, it can be observed that the values of ΔG°_{ads} are less than -20 $kJ\ mol^{-1}$ inferring that the benzothiophene inhibitors adsorbed on the surface of the metal by a physical adsorption process. The exception was inhibitor B5, which had a value between the interval of -20 and -40 $kJ\ mol^{-1}$, which suggests the inhibitor was adsorbed on the metal surface by both the physical and chemical adsorption mechanism [100-102].

Table 4.4 Adsorption and interaction parameters for the adsorption of the benzothiophene molecules on the mild steel surface in 1 M HCl medium.

Inhibitor molecule	K_{ads} $(10^4\ mol^{-1})$	$-\Delta G^{\circ}_{ads}$ $(kJ\ mol^{-1})$
B1	0.66	-14.72
B2	3.2	-18.32
P3	2.3	-17.61
B4	0.93	-15.51
B5	15.8	-21.94

Chapter 5
Conclusion

5.1 Conclusions

The study of 5 benzothiophene inhibitors was done in 1 M HCl solution. The aim was to examine and test the inhibition capabilities and adsorption properties of the inhibitors with mild steel. Methods such as electrochemical, computational, and spectroscopic techniques were used to study the five benzothiophene inhibitors. The inhibitors were divided into two groups, and below are the conclusions of the study.

1. **Tafel analysis**
   The five inhibitors in the study exhibited good inhibition efficiency for mild steel in 1 M HCl, and the following trend was reported:

   - B5 > B2 > B3 > B4 > B1.

   The inhibitors mainly interacted with the metal by using both anodic and cathodic sites (mixed-type inhibitors), with the only exception being B4 which primarily acted as a cathodic inhibitor.

2. **Electrochemical impedance spectroscopy (EIS)**
   All five inhibitors showed competent levels of efficiency for mild steel in 1 M HCl solution, and the following order for the concentration of 500 ppm was observed:

   - B5 > B2 > B3 > B4 > B1.

   The trend of the Tafel analysis and EIS analysis correlated excellently; all the inhibitors showed appreciable levels of solution resistance and exhibited excellent corrosion protection capabilities for the mild steel.

3. **Quantum chemical study**
   The HOMO and LUMO figures of all the benzothiophene inhibitors showed that most of the inhibitors could donate and accept electrons, respectively. The presence of pi-electrons from the double bounded structure of the benzothiophene ring, and vital electron donors such as sulphur and nitrogen enable these inhibitors to donate and receive electrons. The quantum chemical parameters proved that these inhibitors could easily interact with metal to limit corrosion.

4. **Spectroscopic studies**
   The reported FTIR spectral for all the inhibitors showed the inhibitor's interaction with the mild steel surface, alluding to a likely formation of an inhibitor/mild steel complex.

5. **Adsorption isotherms**

The five inhibitors obeyed Langmuir's isotherm with the resultant R^2 values reasonably close to unity. Most of the inhibitors reported high K_{ads} values indicating strong interactions between the inhibitors and the mild steel. Four inhibitors showed ΔG°_{ads} values less than -20 $kj\ mol^{-1}$, which meant they adsorbed on the metal surface through the process of physisorption. The only exception was B5, which had a value between -20 $kj\ mol^{-1}$ to -40 $kj\ mol^{-1}$, indicating that the inhibitor was using a physical and chemical adsorption process to attach on the mild steel surface**.**

6. References

1. Davis, J.R., *Corrosion: Understanding the basics*. 2000: Asm International.
2. Winkleman, A., et al., *Preventing corrosion from wearing our future away.* Advanced Materials & Processes, 2011. **169**(3): p. 26-32.
3. Verma, C., et al., *Sulfur and phosphorus heteroatom-containing compounds as corrosion inhibitors: An overview.* Heteroatom Chemistry, 2018. **29**(4): p. e21437.
4. SINGH, N., *CASE STUDY ON SOME OF THE MAJOR CORROSION CATASTROPHES IN THE HISTORY.*
5. Ahsan, S.A., et al., *Metal fume fever: a review of the literature and cases reported to the Louisiana Poison Control Center.* J La state Med soc, 2009. **161**(6): p. 348-51.
6. Bankole, M.T., et al., *Selected heavy metals removal from electroplating wastewater by purified and polyhydroxylbutyrate functionalized carbon nanotubes adsorbents.* Scientific reports, 2019. **9**(1): p. 1-19.
7. Stupnišek-Lisac, E., A. Gazivoda, and M. Madžarac, *Evaluation of non-toxic corrosion inhibitors for copper in sulphuric acid.* Electrochimica acta, 2002. **47**(26): p. 4189-4194.
8. Spitz, K. and J. Trudinger, *Converting Minerals to Metals: From Ore to Finished Product*, in *Mining and the Environment*. 2019, CRC Press. p. 195-224.
9. Verma, C., et al., *Phthalocyanine, naphthalocyanine and their derivatives as corrosion inhibitors: A review.* Journal of Molecular Liquids, 2021. **334**: p. 116441.
10. Chauhan, D.S., C. Verma, and M. Quraishi, *Molecular structural aspects of organic corrosion inhibitors: Experimental and computational insights.* Journal of Molecular Structure, 2021. **1227**: p. 129374.
11. Mashuga, M.E., *Adsorption, thermodynamic and quantum chemical studies of some ionic liquids as corrosion inhibitors for mild steel in HCl*. 2014, North-West University.
12. Roberge, P.R., *Handbook of corrosion engineering*. 2019: McGraw-Hill Education.
13. Tomashov, N.D., *Passivity and protection of metals against corrosion*. 2012: Springer Science & Business Media.
14. Razavi, R.S., *Recent researches in corrosion evaluation and protection*. 2012: BoD–Books on Demand.
15. Ahmad, Z., *–introduction to corrosion*, in *Principles of corrosion engineering and corrosion control*. 2006, Elsevier. p. 1-8.
16. Ahmad, Z., *Principles of corrosion engineering and corrosion control*. 2006: Elsevier.
17. Habeeb, H.J., et al., *Development of new corrosion inhibitor tested on mild steel supported by electrochemical study.* Results in physics, 2018. **8**: p. 1260-1267.
18. Sedriks, A.J., *Corrosion of stainless steel, 2.* 1996.
19. Sorel, S., *Stanislas Sorel.*
20. Kendig, M. and D.J. Mills, *An historical perspective on the corrosion protection by paints.* Progress in Organic Coatings, 2017. **102**: p. 53-59.
21. Buchheit, R.G., *Corrosion resistant coatings and paints*, in *Handbook of environmental degradation of materials*. 2005, Elsevier. p. 367-385.
22. Zheludkevich, M., et al., *Active protection coatings with layered double hydroxide nanocontainers of corrosion inhibitor.* Corrosion Science, 2010. **52**(2): p. 602-611.
23. Sørensen, P.A., et al., *Anticorrosive coatings: a review.* Journal of coatings technology and research, 2009. **6**(2): p. 135-176.

24. Qian, Y., et al., *The application of anti-corrosion coating for preserving the value of equipment asset in chloride-laden environments: A.* Int. J. Electrochem. Sci, 2015. **10**: p. 10756-10780.
25. Safty, A.E., et al., *Zinc toxicity among galvanization workers in the iron and steel industry.* Annals of the New York Academy of Sciences, 2008. **1140**(1): p. 256-262.
26. Ozturk, F., Z. Evis, and S. Kilic, *Hot-Dip Galvanizing Process.* 2017.
27. Ricco, M., S. Cattani, and C. Signorelli, *Zinc exposure for female workers in a galvanizing plant in Northern Italy.* International Journal of Occupational Medicine and Environmental Health, 2018. **31**(1): p. 113-124.
28. Okpogba, A., et al., *Evaluation of heavy metal levels in blood of cable manufacturing factory workers in Nnewi.* Int J Clin Biochem Res, 2019. **6**(3): p. 430-436.
29. Liu, T., et al., *Effect of fluxes on wettability between the molten Galfan alloy and Q235 steel matrix.* Surface and Coatings Technology, 2018. **337**: p. 270-278.
30. Makhlouf, A.S.H. and Y. Gajarla, *Advances in smart coatings for magnesium alloys and their applications in industry*, in *Advances in Smart Coatings and Thin Films for Future Industrial and Biomedical Engineering Applications*. 2020, Elsevier. p. 245-261.
31. Tang, C.-J., *More Works on waste treatment and process improvement*, in *Membrane-Based Separations in Metallurgy*. 2017, Elsevier. p. 273-290.
32. Pooja, G., et al., *Sustainable approach on removal of toxic metals from electroplating industrial wastewater using dissolved air flotation.* Journal of Environmental Management, 2021. **295**: p. 113147.
33. Veritas, D.N., *Cathodic protection design.* Recommended Practice DNV-RP-B401, 2010.
34. Dolson, F.E. and L.J. Alexander, *Problems in Cathodic Protection [with Discussion].* Journal (American Water Works Association), 1947. **39**(11): p. 1079-1089.
35. Zhao, X.D., J. Yang, and X.Q. Fan. *Review on research and progress of corrosion inhibitors*. in *Applied Mechanics and Materials*. 2011. Trans Tech Publ.
36. Liu, Z., et al., *Transmission electron microscopy observation of corrosion behaviors of platinized carbon blacks under thermal and electrochemical conditions.* Journal of the Electrochemical Society, 2010. **157**(6): p. B906.
37. Rajendrachari, S., *Investigation of electrochemical pitting corrosion by linear sweep voltammetry: A fast and robust approach*, in *Voltammetry*. 2018, IntechOpen.
38. Joshi, P. and D. Sutrave, *Building an arduino based potentiostat and instrumentation for cyclic voltammetry.* J. Appl. Sci. Comput, 2018. **5**(12): p. 163-167.
39. Zhang, X., et al., *Effects of scan rate on the potentiodynamic polarization curve obtained to determine the Tafel slopes and corrosion current density.* Corrosion science, 2009. **51**(3): p. 581-587.
40. Dickinson, E.J. and A.J. Wain, *The Butler-Volmer equation in electrochemical theory: Origins, value, and practical application.* Journal of Electroanalytical Chemistry, 2020. **872**: p. 114145.
41. Kakaei, K., M.D. Esrafili, and A. Ehsani, *Graphene and anticorrosive properties*, in *Interface science and technology*. 2019, Elsevier. p. 303-337.
42. Lasia, A., *Electrochemical impedance spectroscopy and its applications*, in *Modern aspects of electrochemistry*. 2002, Springer. p. 143-248.
43. Deshmukh, K., et al., *Dielectric spectroscopy*, in *Spectroscopic Methods for Nanomaterials Characterization*. 2017, Elsevier. p. 237-299.
44. Macdonald, D.D., *Reflections on the history of electrochemical impedance spectroscopy.* Electrochimica Acta, 2006. **51**(8-9): p. 1376-1388.
45. Barsukov, Y. and J.R. Macdonald, *Electrochemical impedance spectroscopy.* Characterization of materials, 2012. **2**: p. 898-913.

46. Huang, J., et al., *Graphical analysis of electrochemical impedance spectroscopy data in Bode and Nyquist representations.* Journal of Power Sources, 2016. **309**: p. 82-98.
47. Instruments, G., *Basics of electrochemical impedance spectroscopy.* G. Instruments, Complex impedance in Corrosion, 2007: p. 1-30.
48. Rubinson, J.F. and Y.P. Kayinamura, *Charge transport in conducting polymers: insights from impedance spectroscopy.* Chemical Society Reviews, 2009. **38**(12): p. 3339-3347.
49. Wu, B. and N. Yoshikai, *Versatile synthesis of benzothiophenes and benzoselenophenes by rapid assembly of arylzinc reagents, alkynes, and elemental chalcogens.* Angewandte Chemie International Edition, 2013. **52**(40): p. 10496-10499.
50. Matsuzawa, T., T. Hosoya, and S. Yoshida, *One-step synthesis of benzo [b] thiophenes by aryne reaction with alkynyl sulfides.* Chemical science, 2020. **11**(35): p. 9691-9696.
51. Anbar, H.S., et al., *Evaluation of sulfonate and sulfamate derivatives possessing benzofuran or benzothiophene nucleus as inhibitors of nucleotide pyrophosphatases/phosphodiesterases and anticancer agents.* Bioorganic Chemistry, 2020. **104**: p. 104305.
52. Keri, R.S., et al., *An overview of benzo [b] thiophene-based medicinal chemistry.* European journal of medicinal chemistry, 2017. **138**: p. 1002-1033.
53. Miao, Y.-h., et al., *Natural source, bioactivity and synthesis of benzofuran derivatives.* RSC advances, 2019. **9**(47): p. 27510-27540.
54. Liu, D., et al., *Adsorption structures of heterocyclic sulfur compounds on Cu (I) Y zeolite: a first principle study*, in *Studies in surface science and catalysis*. 2007, Elsevier. p. 1699-1704.
55. Goyal, M., et al., *Organic corrosion inhibitors for industrial cleaning of ferrous and non-ferrous metals in acidic solutions: A review.* Journal of Molecular Liquids, 2018. **256**: p. 565-573.
56. Brycki, B.E., et al., *Organic corrosion inhibitors.* Corrosion inhibitors, principles and recent applications, 2018. **3**: p. 33.
57. Pearson, R.G., *Hard and soft acids and bases, HSAB, part II: Underlying theories.* Journal of Chemical Education, 1968. **45**(10): p. 643.
58. Parr, R.G. and R.G. Pearson, *Absolute hardness: companion parameter to absolute electronegativity.* Journal of the American chemical society, 1983. **105**(26): p. 7512-7516.
59. Umoren, S. and M. Solomon, *Effect of halide ions on the corrosion inhibition efficiency of different organic species–A review.* Journal of Industrial and Engineering Chemistry, 2015. **21**: p. 81-100.
60. Umoren, S., I. Obot, and E. Ebenso, *Corrosion inhibition of aluminium using exudate gum from Pachylobus edulis in the presence of halide ions in HCl.* E-journal of Chemistry, 2008. **5**(2): p. 355-364.
61. Achutha, K., et al., *Corrosion inhibition of 6061 Al alloy/SiCp composite in HCl medium using 3-chloro-1-benzothiophene-2-carbohydrazide.* Ind J. Chem. Technol., 2011. **18**: p. 439-445.
62. Gece, G., *The use of quantum chemical methods in corrosion inhibitor studies.* Corrosion science, 2008. **50**(11): p. 2981-2992.
63. Arslan, T., et al., *Quantum chemical studies on the corrosion inhibition of some sulphonamides on mild steel in acidic medium.* Corrosion Science, 2009. **51**(1): p. 35-47.
64. Geerlings, P., F. De Proft, and W. Langenaeker, *Conceptual density functional theory.* Chemical reviews, 2003. **103**(5): p. 1793-1874.
65. Koch, G.H., M.P. Brongers, and N.G. Thompson, *Cost of Corrosion and Prevention Strategies in United States*. 2001, CC Technologies Laboratories, Inc.
66. Tüzün, B. and J. Bhawsar, *Quantum chemical study of thiaozole derivatives as corrosion inhibitors based on density functional theory.* Arabian Journal of Chemistry, 2021. **14**(2): p. 102927.
67. Shahraki, M., M. Dehdab, and S. Elmi, *Theoretical studies on the corrosion inhibition performance of three amine derivatives on carbon steel: Molecular dynamics simulation and density functional theory approaches.* Journal of the Taiwan Institute of Chemical Engineers, 2016. **62**: p. 313-321.

68. Saha, S.K., et al., *Density functional theory and molecular dynamics simulation study on corrosion inhibition performance of mild steel by mercapto-quinoline Schiff base corrosion inhibitor.* Physica E: Low-dimensional systems and nanostructures, 2015. **66**: p. 332-341.
69. Popova, A., et al., *AC and DC study of the temperature effect on mild steel corrosion in acid media in the presence of benzimidazole derivatives.* Corrosion science, 2003. **45**(1): p. 33-58.
70. Popova, A., *Temperature effect on mild steel corrosion in acid media in presence of azoles.* Corrosion Science, 2007. **49**(5): p. 2144-2158.
71. Lowmunkhong, P., D. Ungthararak, and P. Sutthivaiyakit, *Tryptamine as a corrosion inhibitor of mild steel in hydrochloric acid solution.* Corrosion Science, 2010. **52**(1): p. 30-36.
72. Döner, A., et al., *Experimental and theoretical studies of thiazoles as corrosion inhibitors for mild steel in sulphuric acid solution.* Corrosion Science, 2011. **53**(9): p. 2902-2913.
73. Eliaz, N., *Corrosion of metallic biomaterials: A review.* Materials, 2019. **12**(3): p. 407.
74. Li, W., et al., *Adsorption and inhibition behavior of 3-chloro-6-mercaptopyridazine towards copper corrosion in sulfuric acid.* Journal of Molecular Liquids, 2022. **357**: p. 119100.
75. Frankel, G., *Fundamentals of corrosion kinetics.* Active protective coatings, 2016: p. 17-32.
76. Popova, A., et al., *Adsorption and inhibitive properties of benzimidazole derivatives in acid mild steel corrosion.* Corrosion science, 2004. **46**(6): p. 1333-1350.
77. Abdulazeez, I., et al., *Mechanistic studies of the influence of halogen substituents on the corrosion inhibitive efficiency of selected imidazole molecules: A synergistic computational and experimental approach.* Applied Surface Science, 2019. **471**: p. 494-505.
78. Zhang, W., et al., *Halogen-substituted acridines as highly effective corrosion inhibitors for mild steel in acid medium.* The Journal of Physical Chemistry C, 2018. **122**(44): p. 25349-25364.
79. Gong, W., et al., *Halogen-substituted thiazole derivatives as corrosion inhibitors for mild steel in 0.5 M sulfuric acid at high temperature.* Journal of the Taiwan Institute of Chemical Engineers, 2019. **97**: p. 466-479.
80. Bonora, P.L., F. Deflorian, and L. Fedrizzi, *Electrochemical impedance spectroscopy as a tool for investigating underpaint corrosion.* Electrochimica acta, 1996. **41**(7-8): p. 1073-1082.
81. Daoud, D., et al., *Adsorption and corrosion inhibition of new synthesized thiophene Schiff base on mild steel X52 in HCl and H2SO4 solutions.* Corrosion science, 2014. **79**: p. 50-58.
82. Zarrouk, A., et al., *Thermodynamic study of metal corrosion and inhibitor adsorption processes in copper/N-1-naphthylethylenediamine dihydrochloride monomethanolate/nitric acid system: part 2.* Research on Chemical Intermediates, 2012. **38**(7): p. 1655-1668.
83. Leth-Olsen, H. *CO2 Corrosion of Steel in Formate Brines for Well Applications*. in *CORROSION 2004*. 2004. OnePetro.
84. Sedik, A., et al., *Dardagan Fruit extract as eco-friendly corrosion inhibitor for mild steel in 1 M HCl: Electrochemical and surface morphological studies.* Journal of the Taiwan Institute of Chemical Engineers, 2020. **107**: p. 189-200.
85. Mashuga, M.E., et al., *Aminomethylpyridazine isomers as corrosion inhibitors for mild steel in 1 M HCl: Electrochemical, DFT and Monte Carlo simulation studies.* Journal of Molecular Liquids, 2021. **344**: p. 117882.
86. Pognon, G., T. Brousse, and D. Bélanger, *Effect of molecular grafting on the pore size distribution and the double layer capacitance of activated carbon for electrochemical double layer capacitors.* Carbon, 2011. **49**(4): p. 1340-1348.
87. Zulkifli, F., et al., *Henna leaves extract as a corrosion inhibitor in acrylic resin coating.* Progress in Organic Coatings, 2017. **105**: p. 310-319.
88. Obot, I. and U.M. Edouk, *Benzimidazole: Small planar molecule with diverse anti-corrosion potentials.* Journal of Molecular Liquids, 2017. **246**: p. 66-90.

89. Hassan, A., et al., *Density functional theory investigation of some Pyridine Dicarboxylic acids derivatives as corrosion inhibitors.* Int. J. Electrochem. Sci, 2020. **15**: p. 4274-4286.
90. Verma, C., et al., *L-Proline-promoted synthesis of 2-amino-4-arylquinoline-3-carbonitriles as sustainable corrosion inhibitors for mild steel in 1 M HCl: experimental and computational studies.* RSC advances, 2015. **5**(104): p. 85417-85430.
91. Zhang, J., et al., *Molecular modeling of the inhibition mechanism of 1-(2-aminoethyl)-2-alkyl-imidazoline.* Corrosion Science, 2010. **52**(6): p. 2059-2065.
92. Lebrini, M., et al., *Enhanced corrosion resistance of mild steel in normal sulfuric acid medium by 2, 5-bis (n-thienyl)-1, 3, 4-thiadiazoles: electrochemical, X-ray photoelectron spectroscopy and theoretical studies.* Applied Surface Science, 2007. **253**(23): p. 9267-9276.
93. Granese, S., et al., *The inhibition action of heterocyclic nitrogen organic compounds on Fe and steel in HCl media.* Corrosion Science, 1992. **33**(9): p. 1439-1453.
94. Ebenso, E.E., et al., *Electrochemical and quantum chemical investigation of some azine and thiazine dyes as potential corrosion inhibitors for mild steel in hydrochloric acid solution.* Industrial & engineering chemistry research, 2012. **51**(39): p. 12940-12958.
95. Ustamehmetoglu, B., F. Demir, and E. Sezer, *Electrochemical copolymerization of benzothiophene with thiophene.* Progress in Organic Coatings, 2013. **76**(11): p. 1515-1521.
96. Lingegowda, D.C., et al., *FTIR spectroscopic studies on cleome gynandra-Comparative analysis of functional group before and after extraction.* Romanian Journal of Biophysics, 2012. **22**(3-4): p. 137-143.
97. Rayner-Canham, G. and D. Sutton, *Identification of ν (N= N) in Metal Arylazo Complexes: The Infrared and Raman Spectra of some Arylazo Complexes of Rhodium (III).* Canadian Journal of Chemistry, 1971. **49**(24): p. 3994-3996.
98. Eddy, N.O., et al., *GCMS studies on Anogessus leocarpus (Al) gum and their corrosion inhibition potential for mild steel in 0.1 M HCl.* International Journal of Electrochemical Sciences, 2011. **6**: p. 5815-5829.
99. Ahdno, H. and H. Jafarizadeh-Malmiri, *Clarification of date syrup by activated carbon: investigation on kinetics, equilibrium isotherm, and thermodynamics of interactions.* International Journal of Food Engineering, 2015. **11**(5): p. 651-658.
100. Obot, I., et al., *Experimental and theoretical investigations of adsorption characteristics of itraconazole as green corrosion inhibitor at a mild steel/hydrochloric acid interface.* Research on Chemical Intermediates, 2012. **38**(8): p. 1761-1779.
101. Onen, A.I., et al., *Titanium (IV) oxide as corrosion inhibitor for aluminium and mild steel in acidic medium.* Int. J. Electrochem. Sci, 2010. **5**(15631573): p. 53.
102. Noor, E.A. and A.H. Al-Moubaraki, *Thermodynamic study of metal corrosion and inhibitor adsorption processes in mild steel/1-methyl-4 [4'(-X)-styryl pyridinium iodides/hydrochloric acid systems.* Materials Chemistry and Physics, 2008. **110**(1): p. 145-154.